THE GEOLOGICAL SOCIETY OF AMERICA®

# Growth and evolution of Neoarchean–Paleoproterozoic crust in the NW Wyoming Province: Evidence from zircon U-Pb age and Lu-Hf isotopes of the Montana metasedimentary terrane

**Tsai-Wei Chen[1,†], Jeffrey D. Vervoort[1], and Julia A. Baldwin[2]**
[1]*School of the Environment, Washington State University, Pullman, Washington 99164, USA*
[2]*Department of Geosciences, University of Montana, Missoula, Montana 59812, USA*

## ABSTRACT

**The Montana metasedimentary terrane in the northern Wyoming Province provides valuable insight into crustal formation and reworking processes along the cratonic margin and offers a unique opportunity to decipher the complex Neoarchean–Paleoproterozoic terrane assembly in southwestern Laurentia. We report new zircon U-Pb dates and Hf isotopes from seven metaigneous samples in the northwestern Montana metasedimentary terrane. The internal textures of zircon in this study are complex; some lack inherited cores and metamorphic overgrowths, while others exhibit core-rim relationships. Based on the cathodoluminescence (CL) features, we interpret these grains to be magmatic populations. These data demonstrate discrete igneous pulses at 2.7 Ga, 2.4 Ga, and 1.7 Ga, which indicate significant crustal formation intervals in the Montana metasedimentary terrane. Zircons at 2.7 Ga have positive $\varepsilon_{Hf}$ values (+2.4 to +0.9) that indicate a depleted mantle source. Most 2.4 Ga and 1.7 Ga samples have negative $\varepsilon_{Hf}$ values (−1.6 to −15.5), which indicate significant contributions from preexisting crust. Two 1.7 Ga samples, however, have near-chondritic $\varepsilon_{Hf}$ values (+0.4 to +0.3) that indicate larger juvenile contributions. The time-integrated Hf isotope trend suggests that the Paleoproterozoic zircons were produced from a mixture of older crust and juvenile mantle inputs. Additionally, the isotopic age fingerprint of the Montana metasedimentary terrane suggests that it differs from northern-bounding terranes. Viewed more broadly, the 2.7 Ga and 1.7 Ga age peaks that the Montana metasedimentary terrane shares with the global zircon age spectrum suggest that the drivers of these events in the Montana metasedimentary terrane were common throughout the Earth and may be associated with the assembly of supercontinents Kenorland and Nuna.**

## INTRODUCTION

Fundamental to unraveling the process of crustal formation and evolution is knowledge of the nature of ancient continental crust. Although only scarce remnants of Archean–Proterozoic crust remain from a long history of magmatism and metamorphism, the chemical and isotopic record of refractory minerals that have survived over the course of Earth's history could contribute to our understanding of the earlier crust (e.g., Amelin et al., 1999; Wilde et al., 2001). Among various minerals that can be used to address these issues, zircon has gained increased focus in recent years. Because zircon has high U concentration and low Pb diffusivity over a wide range of crustal conditions, it has become a frequently used U-Pb chronometer for complex metamorphic terranes (e.g., Corfu, 1993; Whitehouse et al., 1999). Additionally, the low Lu/Hf ratios and high closure temperature of the Lu-Hf system in zircon make it an ideal time capsule for preserving primary magmatic characteristics (e.g., Patchett, 1983; Amelin et al., 2000). This powerful isotopic couplet provides information on both the timing of mineral (re)crystallization and the crustal-versus-mantle sources of those magmas. Rocks from key Archean and Proterozoic crustal fragments—and the zircon from those rocks—can provide essential information on the processes involved in the origin and evolution of continental crust and, in this way, can help decipher the evolution of the early Earth.

An example of an ancient preserved terrestrial block in North America is the Wyoming Province in parts of Wyoming, Montana, and adjacent states (Fig. 1). The Wyoming Province is well-exposed but little studied relative to other Archean cratons, and it contains important information on the continental formation of Laurentia. Since the boundaries between ancient cratonic cores and young orogens often document crustal assembly processes that include the addition of juvenile materials and reworking of the cratonic lithosphere, of particular interest here is the Montana metasedimentary terrane, which is located at the northwestern margin of the Wyoming Province (Fig. 1).

The Montana metasedimentary terrane can provide important insight into the early crustal dynamics of cratons by addressing some first-order questions: (1) What is the significance of events at 2.7 Ga, 2.4 Ga, and 1.7 Ga that took place in the Montana metasedimentary terrane, and (2) what are the roles of these events in the amalgamation of Laurentia? These three Neoarchean and Paleoproterozoic events have been recognized by multiple radiometric dating methods (e.g., Mueller et al., 2004; Jones, 2008). These events are also significant because they are synchronous with active tectonic periods recorded along other margins of the Wyoming Province (e.g., Mueller and Frost, 2006) and in Precambrian terranes worldwide (e.g., Voice et al., 2011).

These questions should be considered in the broader context of understanding (1) the nature of Neoarchean and Paleoproterozoic events in the Wyoming Province, and (2) the tectonic relationship between the Wyoming Province and surrounding terranes. Two major orogenic events have been identified in the Montana metasedimentary terrane: the 2.52–2.45 Ga Tendoy orogeny (Mueller et al., 2012) and the 1.78–1.72 Ga Big Sky orogeny (Harms et al., 2004). The former has also been referred to as the Beaverhead

Tsai-Wei Chen https://orcid.org/0000-0001-9940-2699
[†]tsai-wei.chen@wsu.edu

*GSA Bulletin*;
published online 13 October 2023

https://doi.org/10.1130/B37160.1; 13 figures; 2 tables; 1 supplemental file.

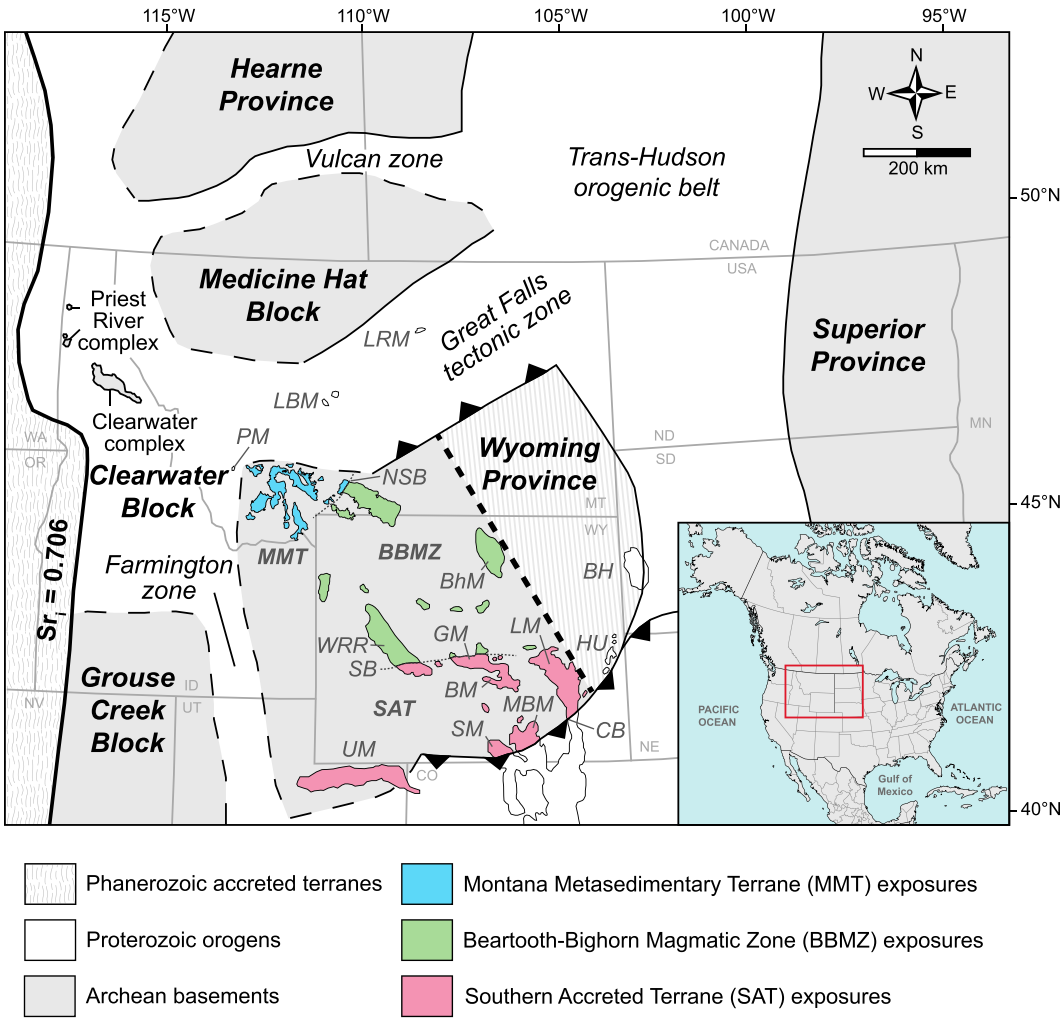


**Figure 1. Overview map of basement terranes of southwestern Laurentia (modified after Foster et al., 2006); the inset map shows the general location of southwestern Laurentia in North America. Margin of juvenile Phanerozoic accreted terranes and Archean basements is approximated by the initial $^{87}Sr/^{86}Sr = 0.706$ line of Armstrong et al. (1977). Light gray shaded areas outline the approximate extension of Archean basements. Exposures of the Clearwater Block are outlined based on Vervoort et al. (2016). Interpreted boundaries of the Wyoming Province are adopted from Bedrosian and Frost (2022). Thick dashed line indicates the eastern boundary of the Wyoming Province proposed by Worthington et al. (2016). The Archean Wyoming Province was exposed principally during Laramide orogeny and can be divided into three subprovinces: Montana metasedimentary terrane (MMT), Beartooth-Bighorn magmatic zone (BBMZ), and Southern accreted terrane (SAT). The Montana metasedimentary terrane was restitched to the Beartooth-Bighorn magmatic zone along the North Snowy Block (NSB) deformation zone, whereas the Southern accreted terrane was sutured to the rest of the province along the Sacawee block (SB). BH—Black Hills; BhM—Bighorn Mountains; BM—Bear Mountain; CB—Cheyenne belt; GM—Granite Mountains; HU—Hartville Uplift; LBM—Little Belt Mountains; LM—Laramie Mountains; LRM—Little Rocky Mountains; MBM—Medicine Bow Mountains; PM—Pioneer Mountains; SM—Sierra Madre; UM—Uinta Mountains; WRR—Wind River Range.**

(e.g., Jones, 2008) and Beaverhead–Tobacco Root orogeny (e.g., Krogh et al., 2011), which is principally recorded in monazite (Cheney et al., 2004; Jones, 2008; Alcock et al., 2013; Cramer, 2015) and zircon (Dahl et al., 2002; Jones, 2008; Krogh et al., 2011; Alcock and Muller, 2012). The later orogenic event was also identified by various chronological methods, including zircon U-Pb (O'Neill et al., 1988; Mueller et al., 2004, 2005; Krogh et al., 2011), monazite U-Pb (Cheney et al., 2004; Gerwin, 2006; Matthews, 2006; Jones, 2008; Alcock et al., 2013; Cramer, 2015), and biotite and amphibole Ar-Ar dating (Harlan et al., 1996; Roberts et al., 2002). Although these events have been known for decades, their tectonic environment, spatial and temporal patterns of deformation—and broad impact on the amalgamation of the supercontinent—are still obscured by pervasive overprinting and metamorphic processes.

In this study, we report whole-rock Lu-Hf isotopic data in conjunction with zircon U-Pb dates and Lu-Hf isotopic data. These zircon U-Pb dates provide a chronologic framework to help unravel the complex magmatic and metamorphic history. Furthermore, the combination of whole-rock and zircon Lu-Hf isotopic data could help shed some light on the nature of the Neoarchean and Paleoproterozoic events and the roles they played in the tectonic assembly of Laurentia. This set of age-related isotopic data allows us to constrain the geological history of the Montana metasedimentary terrane, evaluate the possible plate reconstructions of western Laurentia, as well as provide insight into the global tectonic development of ancient cratons.

## GEOLOGICAL BACKGROUND

The Wyoming Province is an Archean craton that is surrounded by several Precambrian crystalline basement blocks, including the Medicine Hat, Clearwater, and Grouse Creek blocks (Fig. 1). The Medicine Hat Block lies north of the Wyoming Province and is poorly spatially constrained due to pervasive younger sedimentary cover. The few zircon U-Pb dates that have been reported reveal protolith crystallization ages of 3.28–2.50 Ga and later magmatic/metamorphic ages of 1.81–1.76 Ga (Ross et al., 1991; Villeneuve et al., 1993; Davis et al., 1995; Gifford et al., 2020). Some workers have argued that the Medicine Hat Block shares a similar history with the Wyoming Province based on seismic and isotopic data (Henstock et al., 1998; Gifford

et al., 2020), while others have proposed that the two blocks are distinct (Clowes et al., 2002; LaDouceur et al., 2017). To the south and west of the Medicine Hat Block, the Clearwater Block occurs as scattered Archean and Proterozoic basement exposures (i.e., the Clearwater complex and Priest River complex; Doughty et al., 1998; Vervoort et al., 2016; Wang et al., 2022). Sims et al. (2004) defined it as a unique basement based on magnetic anomalies but, because of the sparse information on this block, its relationship to the other Precambrian terranes is very poorly constrained. In the Clearwater Block, two crustal formation ages have been identified by zircon U-Pb geochronology to have occurred in narrow windows at 2.66 Ga and 1.86 Ga (Vervoort et al., 2016; Wang et al., 2022). To the south, the Grouse Creek Block is situated at the western limit of Laurentia and is separated from the Wyoming Province by the 2.45 Ga Farmington zone (Foster et al., 2006; Mueller et al., 2011). Zircon U-Pb dating of the basement rocks in the Grouse Creek Block yields ages of 2.7–2.5 Ga (Egger et al., 2003; Strickland et al., 2011; Isakson, 2012; A. Stacey, 2023, personal commun.), which confirms the presence of Archean basement in this area.

The Wyoming Province is delineated by three well-constrained margins: the 1.86–1.77 Ga Great Falls tectonic zone in the north; the 1.77–1.72 Ga Trans-Hudson orogenic belt in the east; and the 1.78–1.74 Ga Cheyenne belt in the south (Chamberlain, 1998; Dahl et al., 1999; Mueller et al., 2005; Mueller and Frost, 2006; Fig. 1). The entire province appears to have undergone significant crustal growth at 3.4–3.2 Ga and 2.8–2.6 Ga (e.g., Mogk et al., 1992, 2023; Mueller et al., 1992, 1998; Frost et al., 2006; Grace et al., 2006; Chamberlain and Mueller, 2007, 2019). After a relatively quiescent period from 3.2 Ga to 3.0 Ga, deformation was accompanied by voluminous magmatism and modified the crystalline basement at 3.0–2.8 Ga in the northwestern Wyoming Province and at 2.7–2.5 Ga in the southern province (Mueller and Frost, 2006; Mogk et al., 2023). It is thought that these processes led to an unusually viscous and stiff lithospheric mantle of the Wyoming Province (e.g., Mueller and Frost, 2006), which formed a stable and long-lived subcontinental mantle root, making this lithosphere resistant to destruction by later tectonic processes. Following cratonization and subsequent stability, the Wyoming Province rifted and was modified during a period of Proterozoic extension at 2.2–2.0 Ga (Premo and Van Schmus, 1989; Cox et al., 2000; Mueller et al., 2004; Harms and Baldwin, 2023). At 1.9–1.7 Ga, the Wyoming Province amalgamated with the Superior Province and the Medicine Hat Block along the Trans-Hudson orogenic belt and the Great Falls tectonic zone (Dahl et al., 1999; Mueller et al., 2005; Mueller and Frost, 2006), respectively. The incorporation of these terranes into Laurentia eventually assembled the geological nucleus of North America (e.g., Whitmeyer and Karlstrom, 2007).

Based on differences in ages and isotopic compositions in the late Archean, the Wyoming Province can be divided into three subprovinces. From north to south, these are the Montana metasedimentary terrane, the Beartooth-Bighorn magmatic zone, and the Southern accreted terrane (Fig. 1). The Southern accreted terrane is composed of late Archean supracrustal sequences and is characterized by Neoarchean magmatic and tectonic activity. Zircon and titanite U-Pb dating suggest that major magmatic events in the Southern accreted terrane occurred in pulses during 2.7–2.5 Ga (Ludwig and Stuckless, 1978; Verts et al., 1996; Chamberlain et al., 2003; Frost et al., 2006; Grace et al., 2006). These magmatic activities have been interpreted as the addition of juvenile material to the older cratonic block based on their geochemical characteristics (Frost et al., 1998).

North of the Southern accreted terrane, the Beartooth-Bighorn magmatic zone in the central Wyoming Province is predominantly made up of the 3.5–2.9 Ga trondhjemite-tonalite-granodiorite (TTG) association and a 2.8 Ga granitic gneiss suite that underwent variable degrees of deformation and metamorphism (Mueller et al., 1988, 2010, 2014; Frost and Fanning, 2006; Mueller et al., 2014; Frost et al., 2017). Evidence of Eoarchean crust in the Beartooth-Bighorn magmatic zone is supported by 3.8–3.6 Ga zircon xenocrysts in layered gneiss (Frost et al., 2017), ca. 3.8 Ga Nd model ages in trondhjemitic gneiss (Mueller et al., 1996), and detrital zircon U-Pb ages of up to 3.96 Ga in quartzite (Mueller et al., 1992). In the southern Beartooth-Bighorn magmatic zone, the Oregon Trail structural belt, extending east to west, represents the southernmost exposures of the Beartooth-Bighorn magmatic zone. The Oregon Trail structural belt marks the southern limit of the 2.8 Ga magmatic record in the central province (Chamberlain et al., 2003). The boundary of the Beartooth-Bighorn magmatic zone and the Southern accreted terrane is obscured in the field due to a lack of structural data in the southern Beartooth-Bighorn magmatic zone. Bedrosian and Frost (2022) used "$\varepsilon_{Nd} = -4$" to estimate the location of the boundary because the initial Nd composition of the Beartooth-Bighorn magmatic zone is less radiogenic than the juvenile Southern accreted terrane. Much of the Beartooth-Bighorn magmatic zone has been undeformed since 2.8 Ga, although its southern margin was reactivated at 2.6 Ga due to its juxtaposition against the Southern accreted terrane (Naylor et al., 1970; Aleinikoff et al., 1989; Frost et al., 1998, 2006, 2016; Chamberlain et al., 2003; Grace et al., 2006). Based on differences in structural styles, geochemical characteristics, and isotopic ages of the Beartooth-Bighorn magmatic zone and Montana metasedimentary terrane, Mogk et al. (1988, 1992) suggested that these two terranes have different origins and distinct geological histories. These authors proposed that the Montana metasedimentary terrane was restitched to the Beartooth-Bighorn magmatic zone along the North Snowy Block deformation zone—a ductile shear zone consisting of several northeast-striking thrust faults—during 2.75–2.55 Ga (Mogk et al., 1988, 1992).

The Great Falls tectonic zone, lying north of the Montana metasedimentary terrane, marks the boundary separating the Wyoming Province from the Medicine Hat Block. This broad zone of faults and lineaments has been argued to record collision between the Wyoming Province and the Medicine Hat Block (O'Neill and Lopez, 1985). Based on the seismic velocity structure, a fossil remnant of a north-dipping slab (Little Belt slab) has been interpreted to exist beneath the Great Falls tectonic zone (e.g., Gorman et al., 2002). Zircon U-Pb dates of 1.86 Ga from the Little Belt Mountains of the Great Falls tectonic zone (Fig. 1), as well as the calc-alkaline affinity of these rocks, may indicate that the collision between terranes occurred in the Paleoproterozoic, which has been called the Great Falls orogeny (Mueller et al., 2002). The peak timing of the collisional event in the eastern part of the Great Falls tectonic zone is estimated to be ~100 m.y. younger than that of the western part of the Great Falls tectonic zone; thus, a two-phase diachronous orogen was suggested following previous studies (e.g., Mueller et al., 2005; Gifford et al., 2018). Bedrosian and Frost (2022) proposed an evolutionary model of the Great Falls orogeny based on geophysical and geochemical data. They argued that the Great Falls orogeny was formed in two phases: The earlier Medicine Hat phase occurred at 1.86–1.80 Ga and involved the incorporation of the Little Belt arc into the Medicine Hat Block and closure of the Medicine Hat Ocean. The later Big Sky phase occurred at 1.80–1.72 Ga and involved the accretion of the Wyoming Province to the Little Belt arc and Medicine Hat Block.

Rocks of the Montana metasedimentary terrane are lithologically and geochemically distinct from other parts of the Wyoming Province. They are characterized by Archean quartzofeldspathic gneisses intercalated with pelite-quartzite-carbonate supracrustal associations and have been metamorphosed to intermediate- to high-metamorphic grade (Mogk et al., 1992, 2004;

Mueller et al., 1993, 1998, 2004). Although much of the Montana metasedimentary terrane is obscured by the sedimentary cover, ~5%–10% of the Precambrian basement was uplifted and exposed during the Laramide orogeny (Late Cretaceous to early Tertiary; Burger, 2004). These exposures encompass the Tobacco Root and Highland mountains, as well as the Northern and Southern Madison, Gallatin, Ruby, Greenhorn, and Gravelly ranges (Fig. 2). In the southern part of the Gravelly and Northern Madison ranges, a northeast–southwest-trending geochronological line named the Giletti's line (Giletti, 1966) was suggested to define a boundary of reset Paleoproterozoic K-Ar and Rb-Sr ages to the northwest and a zone where the ages are not reset to the southeast. The northwestern region of Giletti's line was suggested to document high-grade metamorphism resulting from the collision of the Medicine Hat Block and Wyoming Province, and thus is considered to record crustal thickening and thrusting at the edge of the Wyoming Province (Mueller et al., 2005).

The oldest ages found in the northern Montana metasedimentary terrane are recorded in inherited zircon cores and detrital zircon from the Tobacco Root Mountains (Mueller et al., 1998, 2004; Krogh et al., 2011). The dominant age population of detrital zircon is between 3.4 Ga and 3.2 Ga, which may reflect a major crustal formation event in the northern Wyoming Province. During the Neoarchean, a 2.7 Ga magmatic event formed Archean quartzofeldspathic gneiss precursors in the Ruby and Southern Madison ranges (Mueller et al., 1993; Jones, 2008). These basement rocks record at least two episodes of magmatism and metamorphism. The older event, taking place at 2.52–2.45 Ga and termed the Tendoy orogeny, was identified by the $^{207}Pb$-$^{206}Pb$ step-leaching method for monazite-dominated garnet (Roberts et al., 2002) and further confirmed by U-Pb dates of zircon and monazite separated from gneisses (Dahl et al., 2002; Cheney et al., 2004; Jones, 2008; Krogh et al., 2011; Alcock and Muller, 2012; Alcock et al., 2013; Cramer, 2015). The nature of the Tendoy orogeny is unclear, and has been interpreted as either rift-related magmatism (Roberts et al., 2002; Jones, 2008) or contractional tectonics (Kellogg et al., 2003; Mueller et al., 2012; Harms and Baldwin, 2023). At 2.06 Ga, a swarm of mafic dikes cut across Archean gneisses in the Tobacco Root Mountains, which indicates a rifting event (Mueller et al., 2004). Finally, a major tectonothermal event at 1.78–1.72 Ga, the Big Sky orogeny, is thought to have overprinted the record of the Tendoy orogeny. This widespread orogenic event is recorded by the zircon and monazite U-Pb systems of various lithologies (O'Neill et al., 1988; Roberts et al., 2002; Cheney et al., 2004; Mueller et al., 2004, 2005; Gerwin, 2006; Matthews, 2006; Jones, 2008; Alcock et al., 2013; Cramer, 2015). Additionally,

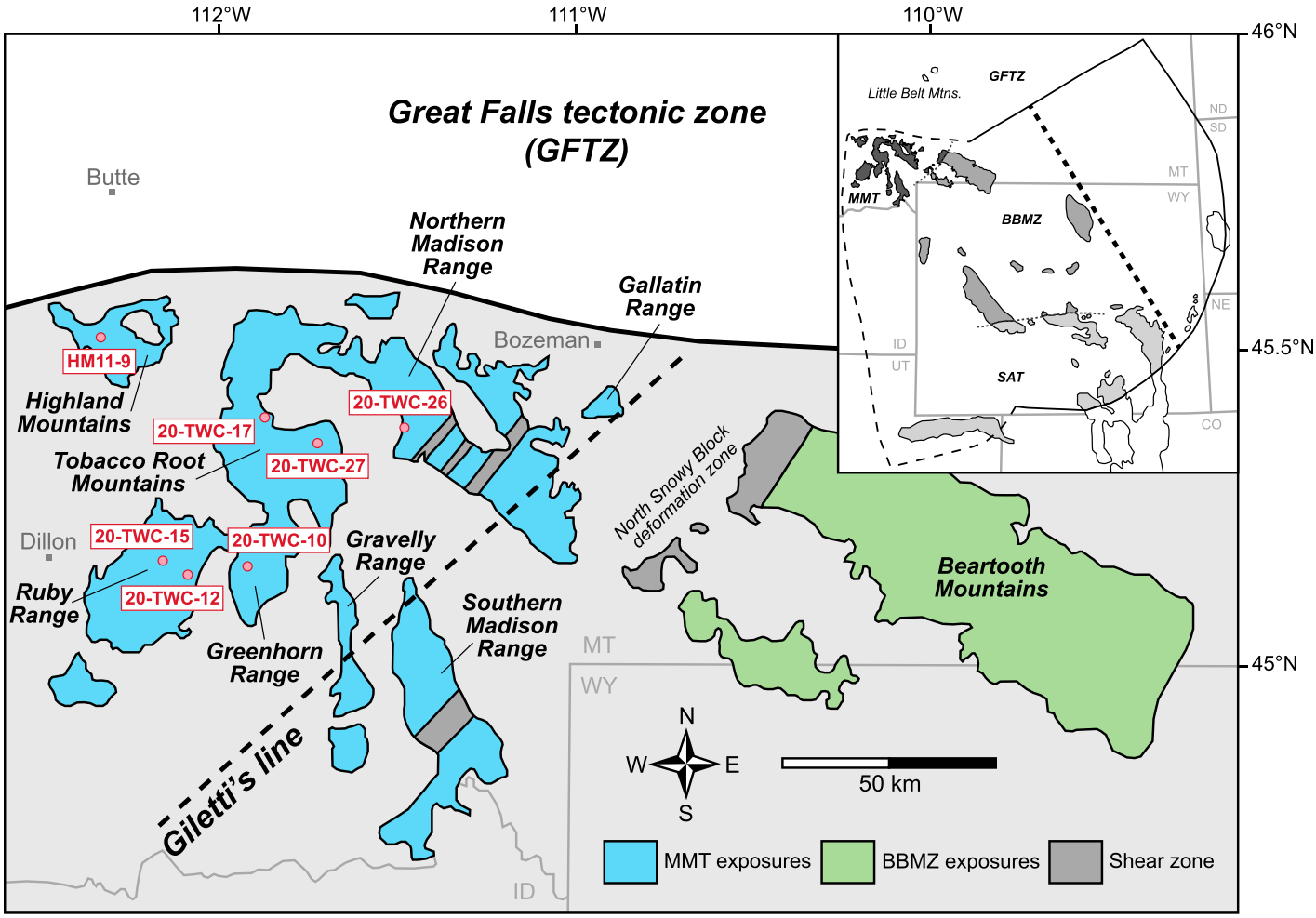


**Figure 2. Map of southwestern Montana showing basement exposures (modified after Mogk et al., 1992) and sample locations. Inset map shows the terrane configuration and interpreted boundaries of the Wyoming Province (solid and thin dashed lines—Bedrosian and Frost, 2022; thick dashed line—Worthington et al., 2016). BBMZ—Beartooth-Bighorn magmatic zone; GFTZ—Great Falls tectonic zone; MMT—Montana metasedimentary terrane; SAT—Southern accreted terrane.**

TABLE 1. SAMPLE LOCATIONS, ROCK TYPES, DATES, AND Hf ISOTOPES

| Sample | Coordinates | | Rock type | Date (Ma)* | Date interpretation | Whole-rock $\varepsilon_{Hf(i)}$† | Zircon $\varepsilon_{Hf(i)}$† |
|---|---|---|---|---|---|---|---|
| | Latitude (N) | Longitude (W) | | | | | |
| Tobacco Root Mountains | | | | | | | |
| 20-TWC-17 | 45°31.737′ | 112°01.066′ | Amphibolite | 1762 ± 10 | Magmatic | +1.1 ± 0.1 | +0.3 ± 2.2 |
| 20-TWC-27 | 45°26.424′ | 111°51.196′ | Quartzofeldspathic gneiss | ~2400 | Magmatic | –8.5 ± 0.1 | –6.0 ± 1.8 |
| | | | | 1733 ± 9 | Magmatic | –18.3 ± 0.1 | –15.5 ± 2.5 |
| Highland Mountains | | | | | | | |
| HM11-9 | 45°40.502′ | 112°35.101′ | Granitic gneiss | 1802 ± 10 | Magmatic | –1.5 ± 0.1 | +0.4 ± 1.9 |
| Northern Madison Range | | | | | | | |
| 20-TWC-26 | 45°27.173′ | 111°39.212′ | Gedrite gneiss | 2433 ± 13 | Magmatic | –17.6 ± 0.1 | –9.2 ± 0.8 |
| | | | | ~1800 | Magmatic | –16.0 ± 0.1 | –14.7 ± 0.9§ |
| Ruby Range | | | | | | | |
| 20-TWC-12 | 45°11.033′ | 112°13.830′ | Amphibolite | 2745 ± 18 | Magmatic | –15.5 ± 0.1 | +0.9 ± 2.0 |
| | | | | 2422 ± 13 | Magmatic | –14.7 ± 0.1 | –1.7 ± 1.8 |
| | | | | 1771 ± 10 | Magmatic | –13.1 ± 0.1 | –10.2 ± 1.9 |
| 20-TWC-15 | 45°13.494′ | 112°17.119′ | Leucogneiss | 2764 ± 15 | Magmatic | –38.8 ± 0.1 | +2.4 ± 2.4 |
| | | | | 2465 ± 13 | Magmatic | –15.4 ± 0.1 | –1.6 ± 2.5 |
| Greenhorn Range | | | | | | | |
| 20-TWC-10 | 45°13.019′ | 112°01.699′ | Amphibolite | 1765 ± 9 | Magmatic | –13.3 ± 0.1 | –13.7 ± 0.7 |

*Reported results are zircon weighted mean $^{207}Pb/^{206}Pb$ dates with errors at the 95% confidence level. Note that the reproducibility of the FC-1 standard was propagated into errors.

†The initial Hf isotopic compositions were calculated using the present-day chondritic uniform reservoir values of $^{176}Hf/^{177}Hf = 0.282785$ and $^{176}Lu/^{177}Hf = 0.0336$ (Bouvier et al., 2008) and $^{176}Lu$ decay constant of $1.867 \times 10^{-11}$ yr$^{-1}$ (Söderlund et al., 2004). Whole-rock data are within-run values with uncertainty given as two standard errors (2SE). Zircon data are mean values with uncertainty given as two standard deviations (2SD) of the population.

§Result is reported as single-grain, within-run value with two standard errors (2SE).

the Big Sky orogeny is considered to have extensively modified the northwestern margin of the Wyoming Province (i.e., Montana metasedimentary terrane) and resulted in upper amphibolite- to lower granulite-facies metamorphism (Harms et al., 2004).

## SAMPLES AND ANALYTICAL METHODS

Seven orthogneiss and amphibolite samples were collected in this study from five basement uplift areas northwest of Giletti's line (Fig. 2). All uplifted basement exposures were metamorphosed to upper amphibolite facies, and most are strongly foliated. Our strategy was to select representative samples based on their rock types, mineral assemblages, and geological contexts to obtain robust zircon U-Pb dates and Hf isotopic compositions. A summary of rock types, dates, and Hf isotopes is given in Table 1. See Supplemental File S1[1] for detailed localities and sample descriptions, and Supplemental File S2 for descriptions of whole-rock major- and trace-element compositions.

### Sample Preparation

Rock samples were crushed and chipped in a jaw crusher, then split and ground into powders using an agate ball mill in the GeoAnalytical Laboratory (GAL) at Washington State University (WSU), Pullman, Washington, USA. We used agate instead of a tungsten-carbide ball mill to avoid $^{180}W$ contamination of the Hf isotopic ratio. Samples were also crushed, disaggregated by electric-pulse disaggregation, and processed by heavy-liquid and magnetic separation techniques at Zirchron LLC in Tucson, Arizona, USA, to separate mineral grains.

### Whole-Rock Lu-Hf Isotope Geochemistry

Whole-rock powders were weighed and poured into high-pressure, steel-jacketed Teflon dissolution vessels (200 mg for each sample) and digested in a 1:10 mixture of concentrated $HNO_3$-HF. The samples were placed in an oven at 160 °C for five to seven days for complete dissolution. Following digestion and subsequent dry down, a 1:2 mixture of $H_3BO_3$ and 6 M HCl was added to samples so that the solid fluoride residues could be converted to soluble chlorides. After conversion into HCl-based solutions, each sample solution was spiked with an enriched $^{176}Lu$-$^{180}Hf$ tracer. After sample-spike equilibration, Lu and Hf were isolated by using two stages of chromatography. Chromatographic separation generally followed the detailed procedure of Johnson et al. (2018). The isotope analyses were performed on a Thermo Scientific Neptune Plus high-resolution multicollector–inductively coupled plasma–mass spectrometer (MC-ICP-MS) in the Radiogenic Isotope and Geochronology Laboratory (RIGL) at WSU. Over the course of measurements, unknowns were bracketed by analyses of standards, and all solutions analyzed in a session were reduced together. Isotopes $^{175}Lu$ and $^{173}Yb$ were measured to correct interference from $^{176}Lu$ and $^{176}Yb$ on $^{176}Hf$; the detailed correction protocol is described in Vervoort et al. (2004). In addition, $^{176}Hf/^{177}Hf$ was also corrected for mass bias exponential law with $^{179}Hf/^{177}Hf$ of 0.7325 (Patchett and Tatsumoto, 1980). Following interference and mass bias corrections, Hf isotopic ratios were normalized to the JMC475 Hf standard with $^{176}Hf/^{177}Hf$ of 0.282160 (Vervoort and Blichert-Toft, 1999). Initial $\varepsilon_{Hf}$ values (parts per $10^4$ deviation of the initial $^{176}Hf/^{177}Hf$ ratios between samples and chondritic uniform reservoir, CHUR), were calculated at the assigned U-Pb age of each sample using a $^{176}Lu/^{177}Hf$ value of 0.0336 and a $^{176}Hf/^{177}Hf$ value of 0.282785 for present-day CHUR (Bouvier et al., 2008), with a $^{176}Lu$-$^{176}Hf$ decay constant of $1.867 \times 10^{-11}$ yr$^{-1}$ (Söderlund et al., 2004).

### Zircon Imaging

Zircon grains with no visible cracks and inclusions were handpicked under a binocular microscope and mounted in epoxy disks, then

[1]Supplemental Material. The supplemental material includes two text files of sample description (Supplemental File S1) and whole-rock geochemistry (Supplemental File S2), one figure of whole-rock trace-element diagrams (Fig. S1), five tables of metadata for laser data (Table S1), U-Pb and Lu-Hf isotopic data for zircon reference materials (Tables S2 and S3), and zircon samples (Tables S4 and S5), as well as one table of whole-rock compositions (Table S6). Please visit https://doi.org/10.1130/GSAB.S.24128538 to access the supplemental material, and contact editing@geosociety.org with any questions.

ground and polished to expose the interiors of grains for in situ analyses. Prior to laser analysis, cathodoluminescence (CL) and backscattered electron (BSE) images were acquired using a JEOL JXA-8500F field-emission microprobe at the WSU GAL to examine the internal structures and compositional heterogeneity of grains.

### Zircon U-Pb Geochronology

Zircons were analyzed by laser ablation–inductively coupled plasma–mass spectrometry (LA-ICP-MS). The U-Pb data were collected at the WSU RIGL using the Analyte Excite 193-nm ArF excimer laser ablation system along with a Thermo Scientific Element 2 high-resolution ICP-MS. Samples were analyzed using the single-stream technique in the first round to examine the complexity of the zircon. The single-stream U-Pb analyses were conducted using a 25-μm-diameter spot with a repetition rate of 8 Hz and a fluence of 5–6 J/cm$^2$. For all other analyses, the laser ablation split-stream (LASS) technique was applied to simultaneously acquire U-Pb dates and Hf isotopic compositions. This approach was performed using a 40-μm-diameter spot with a repetition rate of 10 Hz and a fluence of 6–7 J/cm$^2$. The machine setup was based on Fisher et al. (2014), and the detailed analytical parameters are described in Table S1. In each analytical round, each of 10 unknown analyses was bracketed by four measurements of primary standard and normalized to isotopic ratios of standards. The Plešovice ($^{206}$Pb/$^{238}$U = 0.05368, Sláma et al., 2008) and FC-1 ($^{207}$Pb/$^{206}$Pb = 0.076149, Paces and Miller, 1993) zircon standards were used as the primary reference material and $^{207}$Pb/$^{206}$Pb correction reference material, respectively, whereas the GJ-1 ($^{206}$Pb/$^{238}$U age = 600 Ma, Jackson et al., 2004) and 91500 ($^{207}$Pb/$^{206}$Pb age = 1065.4 Ma, Wiedenbeck et al., 1995) zircon standards were analyzed as secondary reference materials for quality assessment of the data. Data reduction was performed using the Iolite 4.7.1 program with integration selection, background subtraction, isotopic ratio and error calculation, downhole correction (detailed description in Paton et al., 2010), and standard normalization. The U-Pb data were reduced with the VizualAge_UcomPbine data reduction scheme (Chew et al., 2014) of Iolite, which uses a smooth cubic spline to model downhole fractionation. The U-Pb dates of single grains and upper intercept and weighted mean $^{207}$Pb/$^{206}$Pb dates of each age population were reduced by the IsoplotR program (Vermeesch, 2018) using a $^{238}$U/$^{235}$U value of 137.818 (Hiess et al., 2012) and decay constants of $1.551 \times 10^{-10}$ yr$^{-1}$ ($^{238}$U-$^{206}$Pb) and $9.849 \times 10^{-10}$ yr$^{-1}$ ($^{235}$U-$^{207}$Pb) (Jaffey et al., 1971). All U-Pb data were plotted with their internal 2σ precisions. The reproducibility of the Plešovice standard was propagated into errors for reported upper intercept dates and Concordia Age (Ludwig, 1998), while the reproducibility of the FC-1 standard was propagated into errors for weighted mean $^{207}$Pb/$^{206}$Pb dates.

### Zircon Hf Geochemistry

Zircon Hf analyses were performed using the LASS technique with the analytical parameters of laser setup described above. Data were collected at the WSU RIGL using an Analyte Excite 193-nm ArF excimer laser ablation system coupled to a Thermo Scientific Neptune Plus MC-ICP-MS. For zircon Hf analysis, the Plešovice zircon standard ($^{176}$Hf/$^{177}$Hf = 0.282482; Sláma et al., 2008) was used as a primary reference material, whereas the FC-1 ($^{176}$Hf/$^{177}$Hf = 0.282482; Woodhead and Hergt, 2005), GJ-1 ($^{176}$Hf/$^{177}$Hf = 0.282200; Morel et al., 2008), and 91500 ($^{176}$Hf/$^{177}$Hf = 0.282305; Blichert-Toft, 2008) zircon standards served as secondary reference materials for quality control of the data. Data reduction was performed using the in-house customized Hf isotope data reduction scheme of the Iolite 4.7.1 program, and generally followed the approach described in Fisher et al. (2011).

## RESULTS

### Zircon U-Pb Geochronology

Table 1 summarizes the U-Pb results, and Table S4 provides the detailed U/Pb and Th/U ratios. CL images of representative zircon grains are shown in Figure 3. In some cases for Archean and Proterozoic samples, determining whether zircons are magmatic or metamorphic is difficult due to the complex growth history. Generally, magmatic zircons tend to preserve euhedral crystal forms and well-developed growth zoning, while metamorphic zircons commonly grow on preexisting magmatic zircon cores and display chaotic and weak zoning (e.g., Corfu et al., 2003; Rubatto, 2017). Wetherill U-Pb concordia plots are presented with weighted mean dates in Figures 4–6. All dates are shown with errors at a confidence level of 95%. Weighted mean dates reported here are based on $^{207}$Pb/$^{206}$Pb ratios because of this method's better precision and accuracy for dates older than 1000 Ma and higher probabilities of Pb loss for Archean and Proterozoic zircons. Samples examined in this study exhibit various degrees of Pb loss and discordance. Regressions provide well-constrained Archean and Paleoproterozoic upper intercept dates of 2.7 Ga, 2.4 Ga, and 1.7 Ga, which agree with weighted mean $^{207}$Pb/$^{206}$Pb dates. Here, we describe the zircon geochronology of the samples based on the U-Pb systematics.

#### *Samples with a Simple Age Population*

The internal textures of samples 20-TWC-17 and 20-TWC-10 show no evidence of inherited cores or metamorphic overgrowths. Some grains display patchy (e.g., Fig. 3, grain 2) and sector (e.g., Fig. 3, grain 43) zoning. These grains are considered to represent the magmatic population. Both samples exhibit comparatively modest patterns of Pb loss (discordance: 20-TWC-17, −10% to 14%; 20-TWC-10, −3% to 6%). Regressions of U-Pb results for the two samples yield upper intercept dates of 1765 ± 8 Ma (MSWD = 1.5, 20-TWC-17) and 1765 ± 7 Ma (MSWD = 1.7, 20-TWC-10). These dates are consistent with the corresponding weighted mean $^{207}$Pb/$^{206}$Pb dates of 1762 ± 10 Ma (MSWD = 1.5, 20-TWC-17) and 1765 ± 9 Ma (MSWD = 1.7, 20-TWC-10) (Fig. 4).

#### *Samples with a Major Age Population and Other Secondary Ages*

The internal structures of sample HM11-9 show oscillatory zoning (e.g., Fig. 3, grain 16), and sample 20-TWC-26 shows two distinct domains: a brighter rim domain (dated at ca. 1.8 Ga) displaying concentric zoning (e.g., Fig. 3, grain 22), and a darker core domain (dated at ca. 2.4 Ga) displaying weak sector zoning (e.g., Fig. 3, grain 23). Both oscillatory and concentric zoning patterns are typical features of magmatic zircon. In high-grade rocks, metamorphic zircons commonly grow on inherited cores (e.g., Rubatto, 2017), and sample 20-TWC-26 lacks inherited core that is older than 2.4 Ga. Consequently, all of these grains are considered to represent the magmatic population. Both samples identify a major age population and pervasive Pb loss signatures (discordance: HM11-9, −1% to 82%; 20-TWC-26, −4% to 52%). For sample HM11-9, a regression excluding the older zircon grains yields an upper intercept date of 1803 ± 4 Ma (MSWD = 1.6), which is consistent with the weighted mean $^{207}$Pb/$^{206}$Pb date of 1802 ± 10 Ma (MSWD = 1.7; Fig. 5). For sample 20-TWC-26, a regression of the older age population yields an upper intercept date of 2434 ± 6 Ma (MSWD = 1.8), which is also consistent with the weighted mean $^{207}$Pb/$^{206}$Pb date of 2433 ± 13 Ma (MSWD = 1.6; Fig. 5). In addition to the major age populations, both samples have a few grains with U-Pb dates outside of the major peaks. Sample HM11-9 shows older inheritance: two discordant grains with $^{207}$Pb/$^{206}$Pb dates of ca. 2.8 Ga, another discordant grain with a $^{207}$Pb/$^{206}$Pb date of ca. 2.4 Ga,

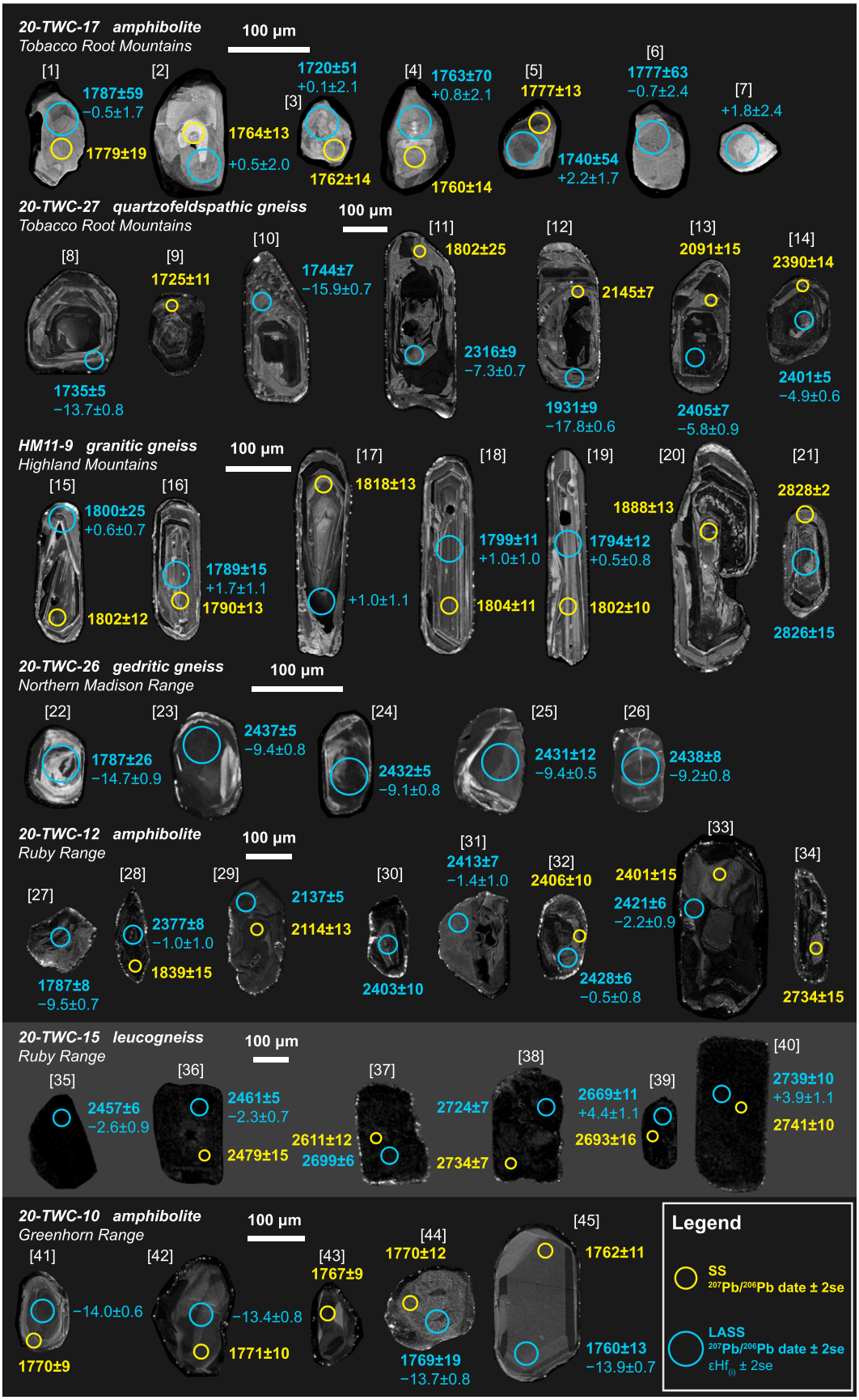


**Figure 3. Representative cathodoluminescence (CL) images of zircon grains from seven metaigneous samples. Smaller yellow circles (25 µm) denote laser ablation spots of single-stream (SS) analyses with $^{207}Pb/^{206}Pb$ dates (±2SE); larger blue circles (40 µm) denote spots of laser ablation split-stream (LASS) analyses with $^{207}Pb/^{206}Pb$ dates (±2SE) and initial $\varepsilon_{Hf}$ values (±2SE). Initial Hf isotopic compositions were calculated at the weighted mean $^{207}Pb/^{206}Pb$ dates reported in Table 1.**

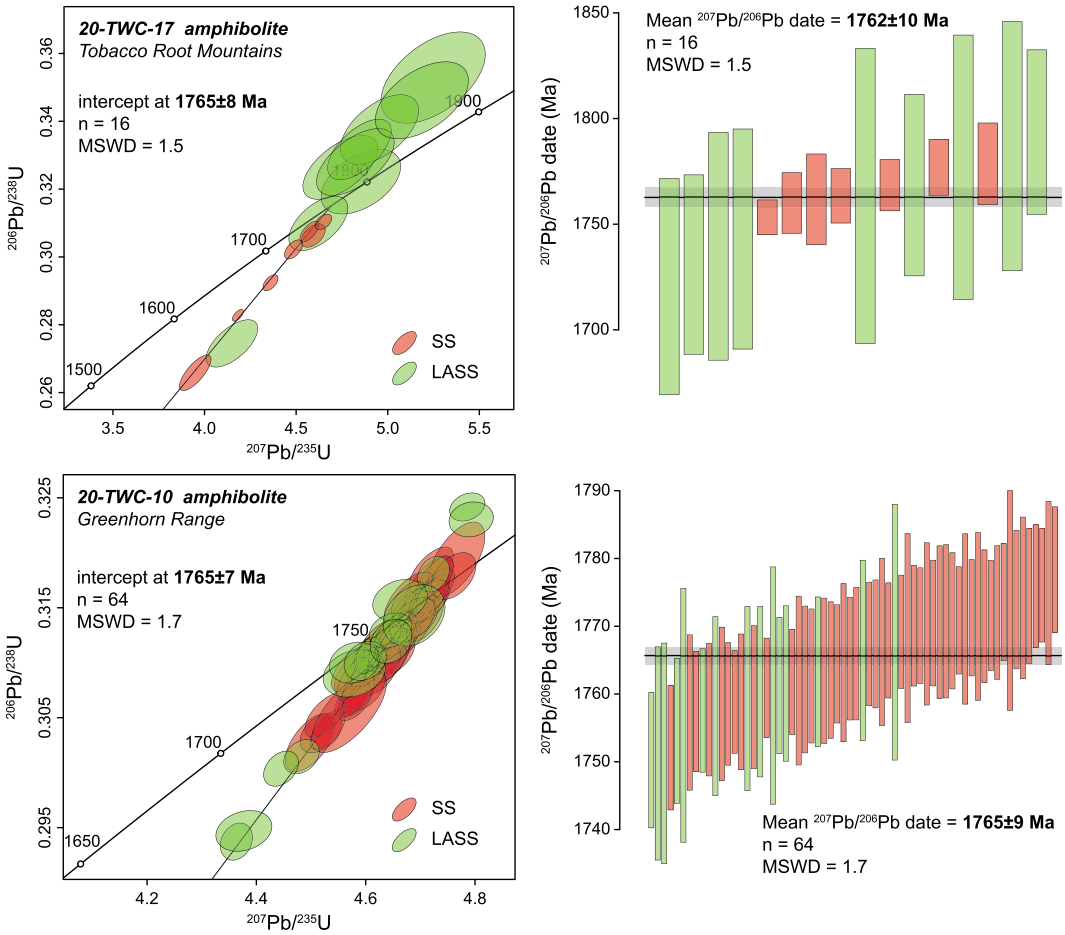


**Figure 4. Wetherill concordia plots and weighted mean $^{207}Pb/^{206}Pb$ dates of zircon U-Pb data for two samples with a simple age population. All uncertainties are presented with errors at the 95% confidence level. Red ellipses (bars) denote laser ablation single-stream (SS) zircon U-Pb analyses; green ellipses (bars) denote laser ablation split-stream (LASS) zircon U-Pb analyses. MSWD—mean squared weighted deviation.**

and a group of grains with $^{207}Pb/^{206}Pb$ dates of between 2.0 Ga and 1.9 Ga, which may represent the mixing of dates between 2.4 Ga and 1.8 Ga components (Fig. 5). In contrast, sample 20-TWC-26 shows younger secondary U-Pb dates: two discordant grains with $^{207}Pb/^{206}Pb$ dates of ca. 1.8 Ga, and several other discordant grains that likely record mixed U-Pb dates of between 2.4 Ga and 1.8 Ga (Fig. 5). It is worth noting that the secondary U-Pb dates in both samples agree with the major age populations in this study (i.e., 2.7 Ga, 2.4 Ga, and 1.7 Ga).

### *Samples with Multiple Age Populations*

The U-Pb data of samples 20-TWC-27, 20-TWC-12, and 20-TWC-15 yield three populations at 2.7 Ga, 2.4 Ga, and 1.7 Ga. The internal structures of these zircon grains are complicated, with some grains displaying core-overgrowth relationships (e.g., Fig. 3, grains 11 and 28). Most 20-TWC-27 grains preserve oscillatory zoning (e.g., Fig. 3, grains 8–14), and a few 20-TWC-12 grains display weak concentric zoning (e.g., Fig. 3, grain 29). These both represent features of magmatic zircon. We carefully selected analysis spots on domains with regular growth zoning. Given that several grains in each population have textures resembling a magmatic growth pattern (e.g., Fig. 3, grains 8, 9, 27, 30, and 34), we consider zircons from both samples to represent the magmatic population. On the other hand, all grains of sample 20-TWC-15 are metamict, and it is difficult to observe their crystalline structures in CL images (Fig. 3, grains 35–40). Based on the prevalence of these ages throughout Ruby Range (e.g., 20-TWC-12), we consider results from this sample to also represent magmatic zircon growth. All three samples demonstrate extreme Pb loss (discordance: 20-TWC-27, −0.1% to 84%; 20-TWC-12, −1% to 82%; 20-TWC-15, −5% to 66%). For sample 20-TWC-27, regressions of the older and younger end members yield upper intercept dates of ca. 2400 Ma and 1733 ± 6 Ma (MSWD = 1.6), respectively. The intercept date of the younger end member is equivalent to its weighted mean $^{207}Pb/^{206}Pb$ date of 1733 ± 9 Ma (MSWD = 1.6; Fig. 6). For sample 20-TWC-12, the oldest population gives a Concordia Age of 2749 ± 10 Ma (MSWD = 2.0), which is consistent with the weighted mean $^{207}Pb/^{206}Pb$ date of 2745 ± 18 Ma (MSWD = 0.4). Additionally, regressions of two younger populations yield upper intercept dates of 2422 ± 6 Ma (MSWD = 1.5) and 1772 ± 10 Ma (MSWD = 1.0), and both are consistent with the weighted mean $^{207}Pb/^{206}Pb$ dates of 2422 ± 13 Ma (MSWD = 1.4) and 1771 ± 10 Ma (MSWD = 1.0; Fig. 6). Several grains from samples 20-TWC-27 and 20-TWC-12 likely record mixed U-Pb dates of between 1.7 Ga and 2.4 Ga, as well as 2.4 Ga and 2.7 Ga end members, and two other grains of sample 20-TWC-27 yield $^{207}Pb/^{206}Pb$ dates of 2.6–2.5 Ga, showing older inheritance (Fig. 6). The U-Pb results of sample 20-TWC-15 show a fan-shaped data field that is bounded by two discordia lines with upper intercept dates of 2764 ± 7 (MSWD = 1.6) and 2465 ± 6 Ma (MSWD = 2.0). These two upper intercept dates are equivalent to their corresponding weighted mean $^{207}Pb/^{206}Pb$ dates of 2764 ± 15 Ma (MSWD = 1.5) and 2465 ± 13 Ma (MSWD = 1.9). The data within the fan-shaped field represent mixed dates or two superimposed patterns of Pb loss (Fig. 6).

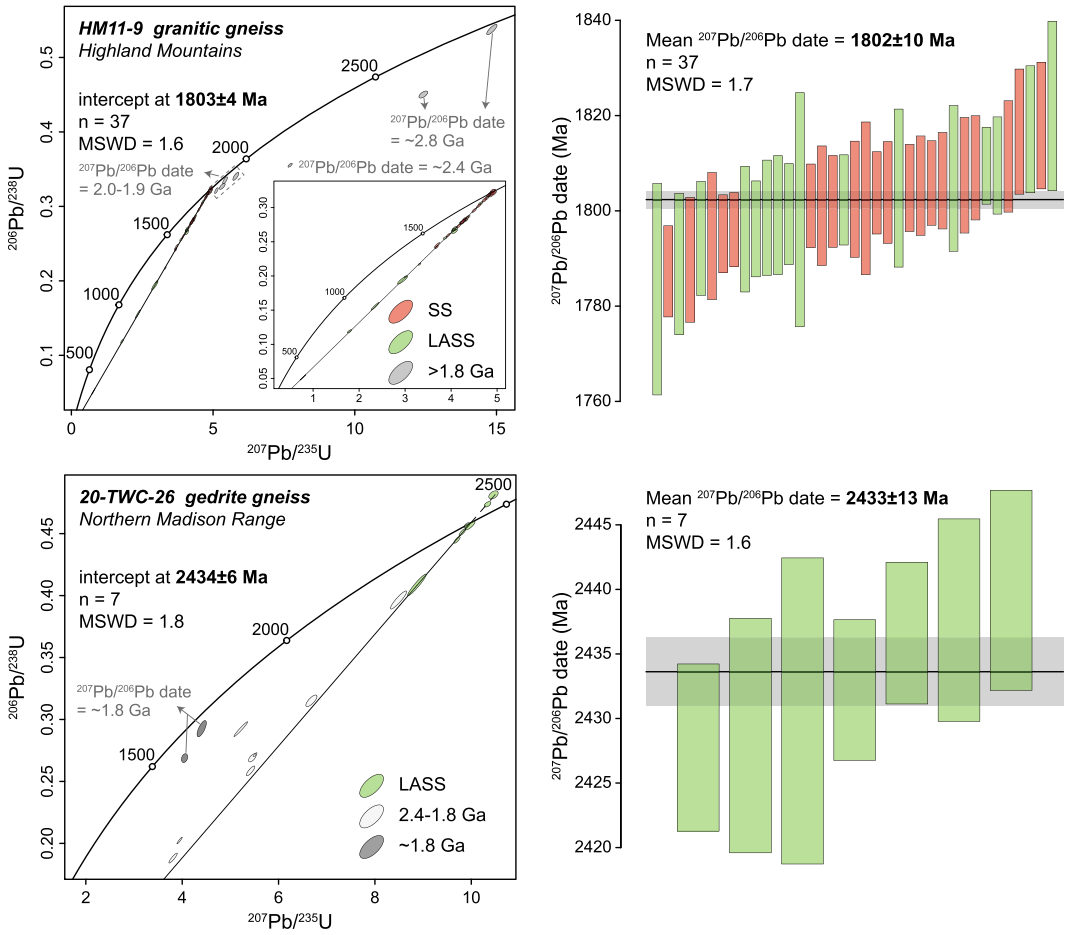


**Figure 5. Wetherill concordia plots and weighted mean $^{207}Pb/^{206}Pb$ dates of zircon U-Pb data for two samples with a major age population and other secondary ages. All uncertainties are presented with errors at the 95% confidence level. Red ellipses (bars) denote laser ablation single-stream (SS) zircon U-Pb analyses; green ellipses (bars) denote laser ablation split-stream (LASS) zircon U-Pb analyses. MSWD—mean squared weighted deviation.**

## Zircon and Whole-Rock Hf Isotope Geochemistry

The Lu-Hf ratios for individual zircon grains are presented in Table S5 and shown in Figures 7–9. A summary of the Lu-Hf isotopic data for bulk rock and zircon is also provided in Tables 1 and 2. The initial Hf isotopic compositions were calculated at the weighted mean $^{207}Pb/^{206}Pb$ date rather than the date of the individual grain to avoid erroneously miscalculating the age of the mixed Hf isotopic compositions (Vervoort and Kemp, 2016). The individual zircon initial $^{176}Hf/^{177}Hf$ and $\varepsilon_{Hf}$ values for each age population broadly overlap and exhibit restricted ranges of Hf isotopic composition. In general, the 2.7 Ga samples are characterized by superchondritic initial $^{176}Hf/^{177}Hf$ ratios, whereas the 2.4 Ga and 1.7 Ga groups are characterized by subchondritic initial $^{176}Hf/^{177}Hf$ ratios. Here, we describe zircon and bulk-rock Lu-Hf isotopes for samples based on the zircon U-Pb systematics. Zircon $^{176}Hf/^{177}Hf$ and $\varepsilon_{Hf}$ values for each sample are reported as the mean, with uncertainty given as two standard deviations (2SD) of the population. Bulk-rock $^{176}Hf/^{177}Hf$ and $\varepsilon_{Hf}$ values are within-run values with uncertainty given as two standard errors (2SE).

### *Samples with a Simple Age Population*

Zircons of sample 20-TWC-17 are characterized by chondritic $(^{176}Hf/^{177}Hf)_{1.76Ga}$ ratios that give a mean $\varepsilon_{Hf\ 1.76Ga}$ value of $+0.3 \pm 2.2$. In contrast, zircons of sample 20-TWC-10 are characterized by subchondritic $(^{176}Hf/^{177}Hf)_{1.77Ga}$ ratios and give a mean $\varepsilon_{Hf\ 1.77Ga}$ value of $-13.7 \pm 0.7$. Bulk-rock compositions of the two samples have initial Hf compositions of $+1.1 \pm 0.1$ (20-TWC-17) and $-13.3 \pm 0.1$ (20-TWC-10), respectively. These values are consistent with their associated mean zircon values.

### *Samples with a Major Age Population and Other Secondary Ages*

The 1.8 Ga zircon population in sample HM11-9 has chondritic $(^{176}Hf/^{177}Hf)_{1.80Ga}$ ratios and a mean $\varepsilon_{Hf\ 1.80Ga}$ value of $+0.4 \pm 1.9$. The bulk-rock composition of this sample has an initial Hf composition of $-1.5 \pm 0.1$, which agrees with the mean zircon value. The older population of sample 20-TWC-26 has subchondritic $(^{176}Hf/^{177}Hf)_{2.43Ga}$ ratios with a mean $\varepsilon_{Hf\ 2.43Ga}$ value of $-9.2 \pm 0.8$. Its bulk rock gives an initial Hf composition of $-17.6 \pm 0.1$ at 2433 Ma, which is much lower than the mean zircon value. However, one single zircon grain from sample 20-TWC-26 has a $^{207}Pb/^{206}Pb$ date of ca. 1800 Ma and a subchondritic $(^{176}Hf/^{177}Hf)_{1.80Ga}$ ratio. This initial Hf ratio gives a $\varepsilon_{Hf\ 1.80Ga}$ value of $-14.7 \pm 0.9$, which is consistent with the bulk-rock $\varepsilon_{Hf\ 1.80Ga}$ value of $-16.0 \pm 0.1$.

### *Samples with Multiple Age Populations*

Sample 20-TWC-27 contains two populations at 2.4 Ga and 1.7 Ga. The older group has a slightly subchondritic $(^{176}Hf/^{177}Hf)_{2.40Ga}$ ratio, which is equivalent to a mean $\varepsilon_{Hf\ 2.40Ga}$ value of $-6.0 \pm 1.8$. The younger group has a less radiogenic $(^{176}Hf/^{177}Hf)_{1.73Ga}$ ratio, equivalent to a mean $\varepsilon_{Hf\ 1.73Ga}$ value of $-15.5 \pm 2.5$. The bulk-rock initial Hf compositions are $-8.5 \pm 0.1$ at 2400 Ma and $-18.3 \pm 0.1$ at 1733 Ma, both of which are slightly lower than their associated mean zircon values. Samples 20-TWC-12 and 20-TWC-15 exhibit three populations at 2.7 Ga, 2.4 Ga, and 1.7 Ga. The 2.7 Ga groups are characterized by superchondritic $(^{176}Hf/^{177}Hf)_{2.7Ga}$ ratios, with mean $\varepsilon_{Hf\ 2.7Ga}$ values of $+0.9 \pm 2.0$ (20-TWC-12) and $+2.4 \pm 2.4$ (20-TWC-15). The 2.4 Ga groups are characterized by slightly

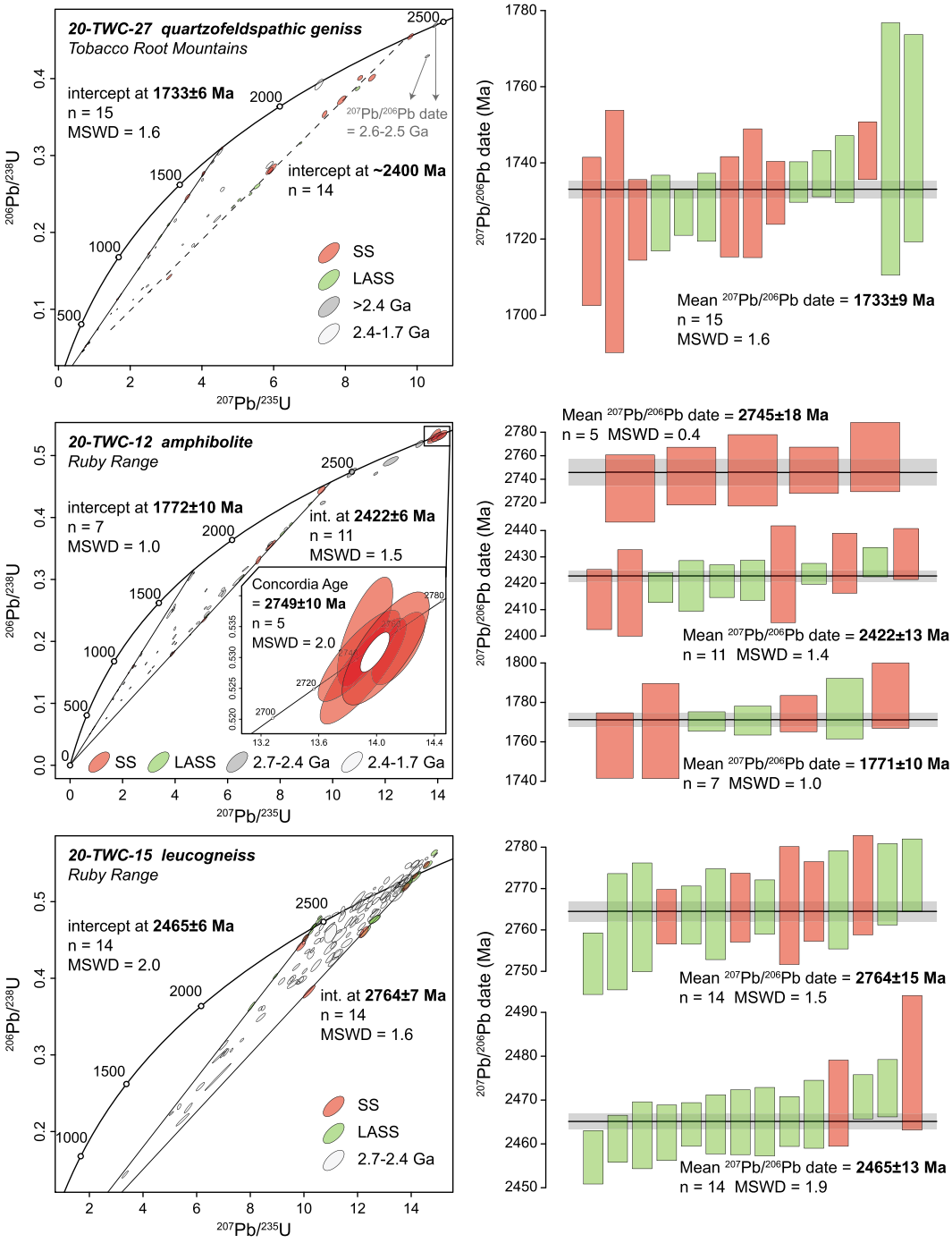


**Figure 6. Wetherill concordia plots and weighted mean $^{207}Pb/^{206}Pb$ dates of zircon U-Pb data for three samples with multiple age populations. All uncertainties are presented with errors at the 95% confidence level. Red ellipses (bars) denote laser ablation single-stream (SS) zircon U-Pb analyses; green ellipses (bars) denote laser ablation split-stream (LASS) zircon U-Pb analyses. MSWD—mean squared weighted deviation.**

subchondritic $(^{176}Hf/^{177}Hf)_{2.4Ga}$ ratios, with mean $\varepsilon_{Hf\ 2.4Ga}$ values of $-1.7 \pm 1.8$ (20-TWC-12) and $-1.6 \pm 2.5$ (20-TWC-15). The bulk-rock initial Hf compositions of these two samples, at 2.7 Ga and 2.4 Ga, disagree with the corresponding mean zircon values; the bulk-rock values (20-TWC-12: $\varepsilon_{Hf\,2.75Ga} = -15.5 \pm 0.1$, $\varepsilon_{Hf\,2.42Ga} = -14.7 \pm 0.1$; 20-TWC-15: $\varepsilon_{Hf\ 2.76Ga} = -38.8 \pm 0.1$, $\varepsilon_{Hf\,2.46Ga} = -15.4 \pm 0.1$) are all significantly less radiogenic than the zircon values. In contrast, the 1.7 Ga zircon population in sample 20-TWC-12 has a subchondritic mean $\varepsilon_{Hf\ 1.77Ga}$ value of $-10.2 \pm 1.9$, which is comparable to the bulk-rock $\varepsilon_{Hf\,1.77Ga}$ value of $-13.1 \pm 0.1$.

## DISCUSSION

### Episodic Growth of Continental Crust in the Montana Metasedimentary Terrane

Previous geochronologic studies have suggested that the oldest portions of the Wyoming Province lie in the Montana metasedimentary terrane and Beartooth-Bighorn magmatic zone (e.g., Mogk et al., 1992; Mueller et al., 1996; Fig. 1). The occurrence of Paleoarchean rocks in the northern Montana metasedimentary terrane is supported by U-Pb dates of 3.4–3.2 Ga detrital zircon in quartzite (Mueller et al., 1998, 2004) and 3.3 Ga inherited zircon in tonalites (Krogh et al., 2011), both in the Tobacco Root Mountains. We were unable, however, to find any zircon population with dates older than 2.8 Ga

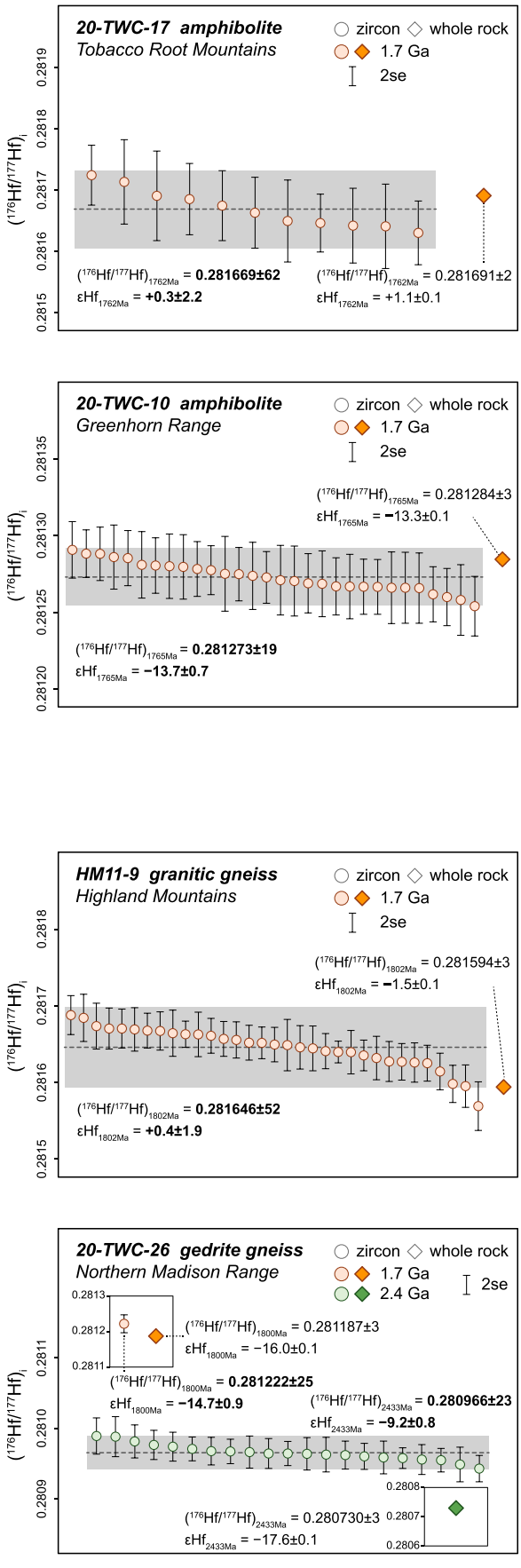


**Figure 7. Initial $^{176}Hf/^{177}Hf$ ratios and $\varepsilon_{Hf}$ values for two samples with a simple age population. Initial Hf isotopic compositions were calculated at the weighted mean $^{207}Pb/^{206}Pb$ dates reported in Table 1. Circles represent zircon; diamonds represent whole rock. Data for individual grains are within-run values with uncertainty given as two standard errors (2SE). Mean values are presented with uncertainty given as two standard deviations (2SD) of the population.**

**Figure 8. Initial $^{176}Hf/^{177}Hf$ ratios and $\varepsilon_{Hf}$ values for two samples with a major age population and other secondary ages. Initial Hf isotopic compositions were calculated at the weighted mean $^{207}Pb/^{206}Pb$ dates reported in Table 1. Circles represent zircon; diamonds represent whole rock. Orange symbols denote sample calculated at 1.7 Ga; green symbols denote sample calculated at 2.4 Ga. Data for individual grains are within-run values with uncertainty given as two standard errors (2SE). Mean values are presented with uncertainty given as two standard deviations (2SD) of the population.**

in samples analyzed as part of this study. The zircon U-Pb data of seven metaigneous samples exposed throughout the Montana metasedimentary terrane provide chronological constraints on the Neoarchean and Paleoproterozoic crustal formation periods and reveal three magmatic pulses with peaks at 2.7 Ga, 2.4 Ga, and 1.7 Ga. This implies episodic growth of continental crust in the Montana metasedimentary terrane during the Neoarchean and Paleoproterozoic.

### *Constraints on the 2.7 Ga Event*

An age of 2.7 Ga was first suggested as the time of metamorphism in the Montana metasedimentary terrane region based on a Rb-Sr isochron date (2750 Ma) from a suite of quartzofeldspathic gneisses from the Tobacco Root Mountains, Northern Madison Range, Gallatin Range, and Ruby Range (James and Hedge, 1980). Roberts et al. (2002), however, argued that the Rb-Sr isochron date is problematic because: (1) the Rb-Sr isochron (James and Hedge, 1980) was based on a suite of rocks collected across four uplifts, in which materials likely have different ages and initial $^{87}Sr/^{86}Sr$ ratios; (2) both Rb and Sr are mobile elements and have open-system behavior during high-grade metamorphism; and (3) sediments are typically rich in water, which promotes elemental mobility. In a later study, Jones (2008) analyzed zircons in migmatitic and granitic gneisses from the Ruby Range, which gave upper intercept dates of 2762 ± 37 Ma, 2772 ± 11 Ma, and 2772 ± 7 Ma. The higher Th/U ratios of zircon cores than those of metamorphic rims indicate a magmatic origin. Thus, he argued that these dates represent the intrusive age of the Ruby Range protolith.

In our study, we documented two samples from the Ruby Range from the oldest (2.7 Ga) population: an amphibolite (20-TWC-12) with a $^{207}Pb/^{206}Pb$ date of 2745 ± 18 Ma and a leucogneiss (20-TWC-15) with a $^{207}Pb/^{206}Pb$ date of 2764 ± 15 Ma (Fig. 6). Although the zircon grains of sample 20-TWC-15 are metamict and do not display clear crystalline structure in their CL images (Fig. 3), the U-Pb data in sample 20-TWC-12 are of magmatic (versus metamorphic) origin based on the interpretation of CL images, which is consistent with the conclusion of Jones (2008). Despite the fact that the original lithology of the protolith of either igneous or sedimentary derivation is hard to constrain in the high-grade metamorphic terrane, the presence of simple age peaks (Fig. 6) rather than wide spectra for these two samples favors an igneous protolith.

In addition to the 2.7 Ga population, we identified two older inherited zircons in a Highland Mountains granitic gneiss (HM11-9, Fig. 5) with $^{207}Pb/^{206}Pb$ dates of ca. 2.8 Ga. These dates may

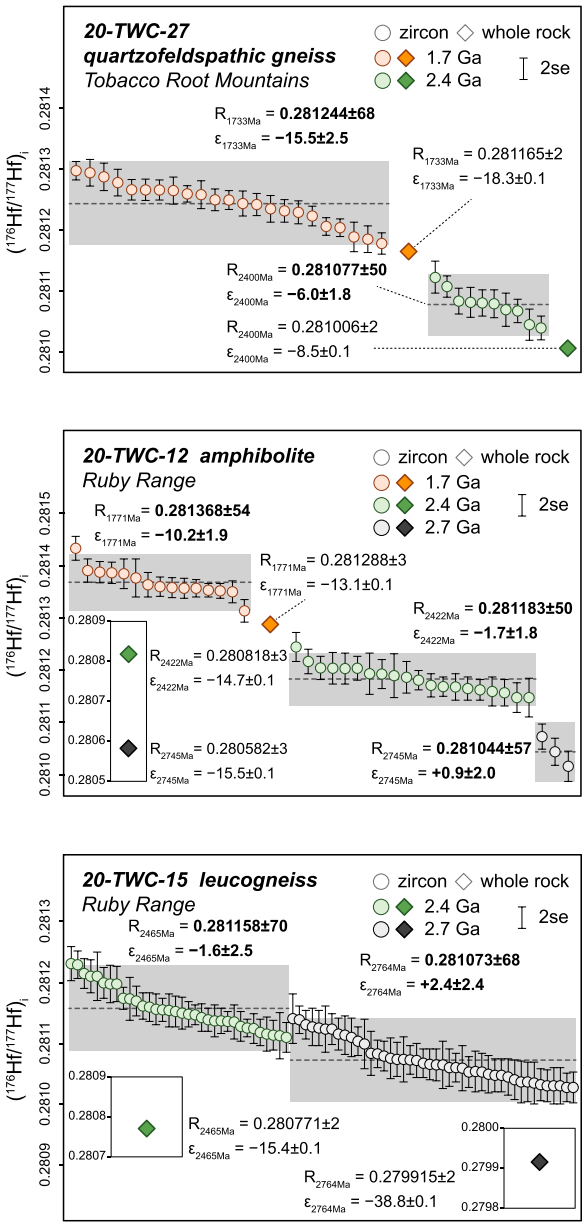


**Figure 9. Initial $^{176}Hf/^{177}Hf$ ratios (R) and $\varepsilon_{Hf}$ values (ε) for three samples with multiple age populations. Initial Hf isotopic compositions were calculated at the weighted mean $^{207}Pb/^{206}Pb$ dates reported in Table 1. Circles represent zircon; diamonds represent whole rock. Orange, green, and gray symbols denote sample calculated at 1.7 Ga, 2.4 Ga, and 2.7 Ga, respectively. Data for individual grains are within-run values with uncertainty given as two standard errors (2SE). Mean values are presented with uncertainty given as two standard deviations (2SD) of the population.**

indicate an event that occurred before 2.7 Ga in the northern Montana metasedimentary terrane or that the Paleoarchean (3.4–3.2 Ga) grains underwent Pb loss during the Neoarchean (2.7 Ga) crustal formation event.

### *Constraints on the 2.4 Ga Event*

Thermochronological analyses of hornblende, biotite, and muscovite from the Madison mylonite zone in the Southern Madison Range provide $^{40}Ar/^{39}Ar$ dates of 2.5–2.4 Ga (Erslev and Sutter, 1990). Erslev and Sutter (1990) interpreted these data to represent the primary cooling history of this area at 2.5 Ga for hornblende and muscovite and 2.4 Ga for biotite. However, it can be challenging to investigate the 2.5–2.4 Ga event through $^{40}Ar/^{39}Ar$ dating north of Giletti's line because the rock suites in this region were thoroughly reset by a later Paleoproterozoic orogenic event at 1.8–1.7 Ga.

Recent U-Pb dating of monazite (Cheney et al., 2004; Jones, 2008; Alcock et al., 2013; Cramer, 2015) and zircon (Dahl et al., 2002; Jones, 2008; Krogh et al., 2011; Alcock and Muller, 2012), however, have confirmed this early Paleoproterozoic event at 2.5–2.4 Ga in the Tobacco Root Mountains and Ruby Range. Dates in the range of 2.52–2.45 Ga were attributed to a tectonothermal event named the Tendoy orogeny (Mueller et al., 2012). Cheney et al. (2004) argued that at 2.4 Ga, monazite from the Tobacco Root Mountains grew during peak metamorphism. Jones (2008) also interpreted these monazite dates to record a high-grade metamorphic event, as evidenced by metamorphic overgrowths on monazite from the Ruby Range. Krogh et al. (2011) inferred that zircons in their samples from the Tobacco Root Mountains represent metamorphic growth, because these grains have equant, multi-faceted, or lath-like morphology, which is typical of metamorphic zircon growth in mafic rocks.

In this study, zircon U-Pb dates recovered from the Northern Madison Range (20-TWC-26, gedrite gneiss), Tobacco Root Mountains (20-TWC-27, quartzofeldspathic gneiss), and Ruby Range (20-TWC-12, amphibolite; 20-TWC-15, leucogneiss) yield Paleoproterozoic dates from 2.47 Ga to 2.40 Ga (Figs. 5 and 6). This range of dates is slightly younger but overlaps with the proposed timing of the Tendoy orogeny. Based on the internal textures, we interpret these grains to represent a magmatic population. Clear evidence, shown in samples 20-TWC-26 and 20-TWC-27, indicates that the 2.4 Ga zircons could not be metamorphic overgrowths because they occur as magmatic cores (e.g., Fig. 3, grains 23 and 25), and some grains even display well-developed magmatic zoning (e.g., Fig. 3, grains 11 and 14). Additionally, simple peaks in the U-Pb age spectrum for samples with a 2.4 Ga population (Figs. 5 and 6) suggest that these zircon grains originated from an igneous protolith. It appears that the Tendoy orogeny was a tectonic process that involved not only regional metamorphism but also magmatism. The common presence of the 2.4 Ga magmatic record in the study area may indicate that the Montana metasedimentary terrane consists of continental fragments that were consolidated during the early Paleoproterozoic.

### *Constraints on the 1.7 Ga Event*

Monazite dates of supracrustal rocks from the Tobacco Root Mountains reveal a prolonged tectonic event that lasted from ca. 1780 Ma to 1720 Ma (Cheney et al., 2004). Harms et al. (2004) attributed this orogenic event to the metamorphism and deformation across the Little Belt, Tobacco Root, and Highland mountains, as well as the Ruby, Northern Madison, and Gallatin ranges in the northern Wyoming Province, which they named the Big Sky orogeny. Previous studies have focused on the deformation and metamorphic records of this orogeny (e.g., Brady et al., 2004; Harms et al., 2004), which suggest that this orogenic event resulted from the collision between the Wyoming Province and Medicine Hat Block along the Great Falls tectonic zone. Zircon and monazite U-Pb dates from the Tobacco Root and Highland mountains southwest of the Great Falls tectonic zone indi-

TABLE 2. SUMMARY OF Lu-Hf ISOTOPIC COMPOSITIONS FOR WHOLE ROCKS

| Sample | Rock type | Lu (ppm) | Hf (ppm) | $^{176}Lu/^{177}Hf$ | $^{176}Hf/^{177}Hf$ | 2SE* | Assigned age (Ma)† | Whole-rock $\varepsilon_{Hf(i)}$§ | Zircon $\varepsilon_{Hf(i)}$§ |
|---|---|---|---|---|---|---|---|---|---|
| Tobacco Root Mountains | | | | | | | | | |
| 20-TWC-17 | Amphibolite | 0.444 | 3.60 | 0.0175 | 0.282276 | ±2 | 1762 | +1.1 ± 0.1 | +0.3 ± 2.2 |
| 20-TWC-27 | Quartzofeldspathic gneiss | 0.991 | 11.4 | 0.0123 | 0.281569 | ±2 | 2400 | –8.5 ± 0.1 | –6.0 ± 1.8 |
| | | | | | | | 1733 | –18.3 ± 0.1 | –15.5 ± 2.5 |
| Highland Mountains | | | | | | | | | |
| HM11-9 | Granitic gneiss | 0.409 | 6.67 | 0.0087 | 0.281892 | ±3 | 1802 | –1.5 ± 0.1 | +0.4 ± 1.9 |
| Northern Madison Range | | | | | | | | | |
| 20-TWC-26 | Gedrite gneiss | 1.18 | 4.49 | 0.0372 | 0.282459 | ±3 | 2433 | –17.6 ± 0.1 | –9.2 ± 0.8 |
| | | | | | | | 1800 | –16.0 ± 0.1 | –14.7 ± 0.9‡ |
| Ruby Range | | | | | | | | | |
| 20-TWC-12 | Amphibolite | 1.94 | 7.41 | 0.0372 | 0.282538 | ±3 | 2745 | –15.5 ± 0.1 | +0.9 ± 2.0 |
| | | | | | | | 2422 | –14.7 ± 0.1 | –1.7 ± 1.8 |
| | | | | | | | 1771 | –13.1 ± 0.1 | –10.2 ± 1.9 |
| 20-TWC-15 | Leucogneiss | 12.5 | 12.1 | 0.1460 | 0.287645 | ±2 | 2764 | –38.8 ± 0.1 | +2.4 ± 2.4 |
| | | | | | | | 2465 | –15.4 ± 0.1 | –1.6 ± 2.5 |
| Greenhorn Range | | | | | | | | | |
| 20-TWC-10 | Amphibolite | 0.162 | 2.34 | 0.0098 | 0.281613 | ±3 | 1765 | –13.3 ± 0.1 | –13.7 ± 0.7 |

*Reported uncertainties of measured ratios are two standard errors (2SE), which are given in the sixth decimal place.
†Reported data were used for initial Hf isotopic composition calculation.
§The initial Hf isotopic compositions were calculated using the present-day chondritic uniform reservoir values of $^{176}Hf/^{177}Hf = 0.282785$ and $^{176}Lu/^{177}Hf = 0.0336$ (Bouvier et al., 2008) and a $^{176}Lu$ decay constant of $1.867 \times 10^{-11}$ yr$^{-1}$ (Söderlund et al., 2004). Whole-rock data are within-run values with uncertainty given as two standard errors (2SE). Zircon data are mean values with uncertainty given as two standard deviations (2SD) of the population.
‡Result is reported as single-grain, within-run value with two standard errors (2SE).

cate that the basement here experienced granulite facies metamorphism at 1.77 Ga (Mueller et al., 2004, 2005), whereas magmatism in the Little Belt Mountains of the Great Falls tectonic zone (Fig. 1) records a zircon U-Pb date of 1.86 Ga. Collectively, Mueller et al. (2005) suggested that peak metamorphic conditions occurred at 1.86 Ga in the eastern Great Falls tectonic zone and at 1.77 Ga in the western Great Falls tectonic zone. The difference in peak metamorphic ages along the Great Falls tectonic zone has led to a model of a two-phase orogen, including an earlier phase at 1.86–1.80 Ga and a later phase at 1.80–1.72 Ga (Bedrosian and Frost, 2022).

In this study, zircon U-Pb dates of five samples from the Tobacco Root Mountains (20-TWC-17, amphibolite; 20-TWC-27, quartzofeldspathic gneiss), Highland Mountains (HM11-9, granitic gneiss), Ruby Range (20-TWC-12, amphibolite), and Greenhorn Range (20-TWC-10, amphibolite) indicate that the Big Sky orogeny in the northwestern Montana metasedimentary terrane began at ca. 1.80 Ga and culminated at ca. 1.76 Ga, which is consistent with the initial and peak timing of the Big Sky phase proposed by Bedrosian and Frost (2022). Zircons dated at 1.7 Ga in all of these samples are interpreted to be of a magmatic population. Based on this evidence and their characteristically simple zircon U-Pb peaks (Figs. 4–6), we argue that these zircons have magmatic origins and were derived from an igneous protolith. The magmatic zircon U-Pb record suggests that significant melt production accompanied the tectonothermal processes during the widespread Big Sky orogeny in the Montana metasedimentary terrane. The zircon U-Pb dates of 1.80–1.76 Ga also confirm the presence of Paleoproterozoic crust of this age in the northwestern Wyoming Province.

### *Age Comparison with Other Subprovinces of the Wyoming Province*

The zircon U-Pb dates define four major magmatic pulses at 3.4–3.2 Ga, 2.8–2.7 Ga, 2.5–2.4 Ga, and 1.8–1.7 Ga in the Montana metasedimentary terrane (Fig. 10), which are interpreted to be associated with crustal formation periods in the northern Wyoming Province. The age peaks in the Montana metasedimentary terrane are different from the patterns in the Beartooth-Bighorn magmatic zone and Southern accreted terrane. The Beartooth-Bighorn magmatic zone is mainly distinguished by ages of ca. 2.1–1.9 Ga and >2.5 Ga (Fig. 10). The Archean dates suggest that a major magmatic pulse produced much of the Archean crust in the central Wyoming Province (e.g., Mueller et al., 1992), whereas the 2.1–1.9 Ga ages may represent the timing of mafic magmatism in the Beartooth-Bighorn magmatic zone associated with supercontinent breakup (Kilian et al., 2016a, 2016b). In the southern Wyoming Province, the Southern accreted terrane shows ages at 2.7–2.5 Ga, 2.4 Ga, and 2.2–2.0 Ga (Fig. 10). The Nd isotopic compositions suggest that the late Archean crust was derived from a juvenile source (Frost et al., 2006), which was followed by mafic magmatism at 2.4 Ga and 2.2–2.0 Ga that was related to mantle plume and rifting activities, respectively (Mammone et al., 2022). The magmatic periods indicated by the three subprovinces of the Wyoming Province show unique features. Compared to the Beartooth-Bighorn magmatic zone and Southern accreted terrane in the southeast, the ca. 2.4 Ga and ca. 1.7 Ga crustal formation periods are distinctive features of the Montana metasedimentary terrane (Fig. 10).

## Nature of the Constituent Neoarchean and Paleoproterozoic Components

The combination of zircon U-Pb age and Hf isotopic data can provide insights into tectonic events and the relationship between igneous activity and crustal evolution. Application of the Hf isotopic system to planetary evolution relies on certain assumptions and observations. These include: (1) the CHUR is representative of bulk Earth composition before planetary differentiation (DePaolo and Wasserburg, 1976); (2) incompatible elements, such as Hf and Nd, are enriched in the crust relative to Lu and Sm, and thus, the depleted mantle (DM) developed higher Lu/Hf and Sm/Nd ratios than the crustal reservoir and undifferentiated body (i.e., CHUR); and (3) large-scale differentiation of Earth's crust and mantle into lasting reservoirs likely occurred no earlier than 3.8 Ga (e.g., Fisher and Vervoort, 2018). Based on these assumptions and observations, as well as the present-day Lu/Hf ratios of the CHUR and DM, we can illustrate the evolution of Hf in this broader context, as shown in Figure 11. Also shown in this figure—to help

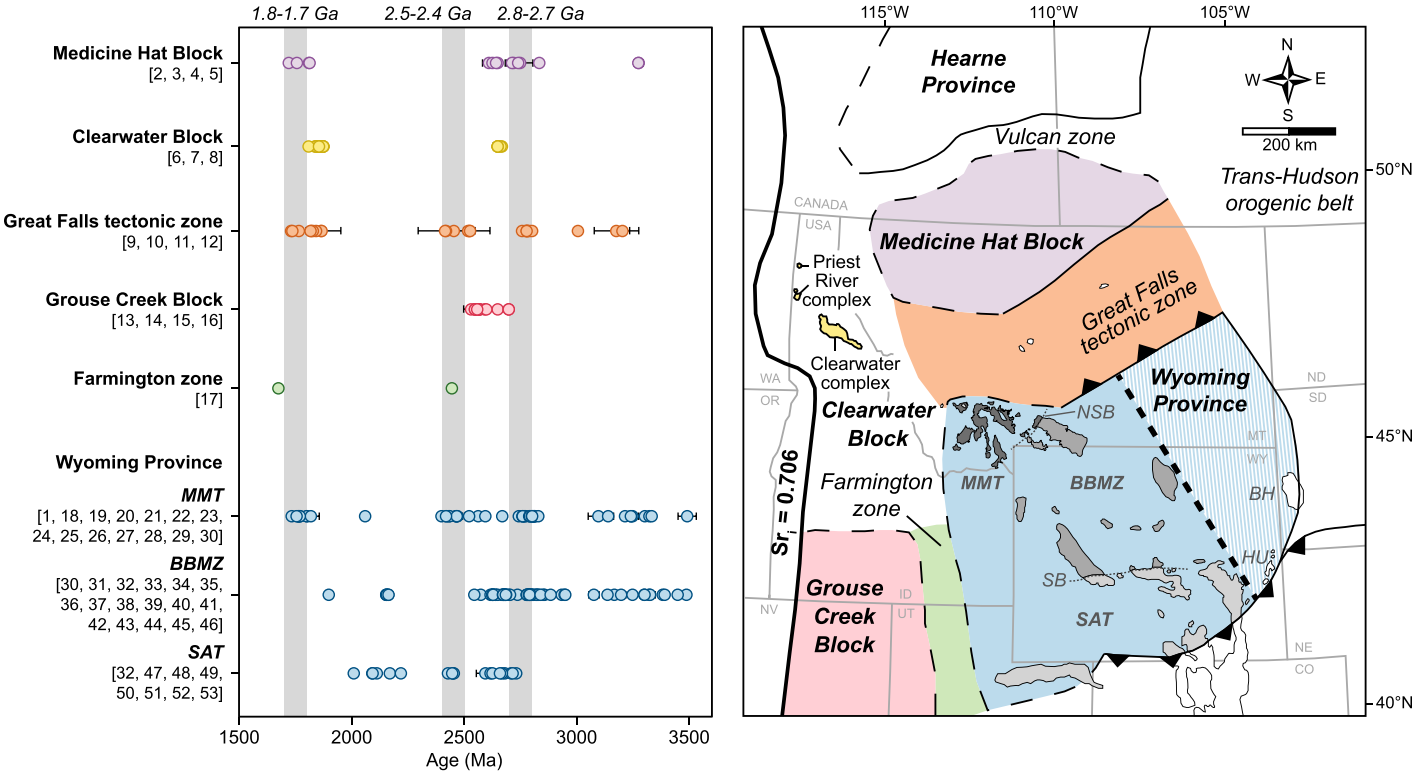


**Figure 10. Zircon U-Pb date compilation for Archean and Proterozoic terranes in southwestern Laurentia. Note that dates from the Black Hills (BH) and Hartville Uplift (HU) were not included here because the basement rocks exposed in these locations may not be parts of the Wyoming Province in some interpretations (e.g., Worthington et al., 2016). BBMZ—Beartooth-Bighorn magmatic zone; MMT—Montana metasedimentary terrane; NSB—North Snowy Block deformation zone; SAT—Southern accreted terrane; SB—Sacawee block. Date references: [1] this study; [2] Ross et al. (1991); [3] Villeneuve et al. (1993); [4] Davis et al. (1995); [5] Gifford et al. (2020); [6] Doughty et al. (1998); [7] Vervoort et al. (2016); [8] Wang et al. (2022); [9] Foster et al. (2006); [10] Mueller et al. (2002); [11] Gifford et al. (2014); [12] Gifford et al. (2018); [13] Egger et al. (2003); [14] Strickland et al. (2011); [15] Isakson (2012); [16] A. Stacey, 2023, personal commun.; [17] Mueller et al. (2011); [18] Mogk et al. (1988); [19] Mogk et al. (1992); [20] Mueller et al. (1993); [21] Mueller et al. (1996); [22] Mueller et al. (1998); [23] Roberts et al. (2002); [24] Dahl et al. (2002); [25] Mueller et al. (2004); [26] Mueller et al. (2005); [27] Jones (2008); [28] Krogh et al. (2011); [29] Alcock and Muller (2012); [30] Mueller et al. (2014); [31] Naylor et al. (1970); [32] Ludwig and Stuckless (1978); [33] Fisher and Stacey (1986); [34] Mueller et al. (1988); [35] Mueller et al. (2010); [36] Aleinikoff et al. (1989); [37] Premo et al. (1990); [38] Zartman and Reed (1998); [39] Frost et al. (1998); [40] Frost and Fanning (2006); [41] Grace et al. (2006); [42] Bagdonas et al. (2016); [43] Frost et al. (2016); [44] Kilian et al. (2016a) (baddeleyite U-Pb); [45] Kilian et al. (2016b) (baddeleyite U-Pb); [46] Frost et al. (2017); [47] Premo and Van Schmus (1989); [48] Verts et al. (1996); [49] Cox et al. (2000); [50] Harlan et al. (2003) (baddeleyite and zircon U-Pb); [51] Bowers and Chamberlain (2006); [52] Frost et al. (2006); [53] Mammone et al. (2022).**

illustrate typical crustal evolution—we show reference lines with Hf isotope evolution of crust separated from the depleted mantle at different times in the past, assuming a $^{176}Lu/^{177}Hf$ ratio of average continental crust ($^{176}Lu/^{177}Hf = 0.015$, Goodge and Vervoort, 2006).

Zircon Hf isotopic compositions in this study have a restricted range of $\varepsilon_{Hf(i)}$ within each sample's age population (i.e., 2.7 Ga, 2.4 Ga, and 1.7 Ga). This homogenous characteristic indicates the absence of open Lu-Hf system behavior in our zircon when viewed at this scale. The 2.7 Ga zircons from the Ruby Range have superchondritic $\varepsilon_{Hf\ 2.7Ga}$ values of $+0.9 \pm 2.0$ (20-TWC-12) and $+2.4 \pm 2.4$ (20-TWC-15), which represent derivation from a less depleted mantle reservoir or possibly some mixture of DM with a small older crustal component.

The age of ca. 2.7 Ga represents one of the main periods of crustal formation in the northwestern Wyoming Province and broadly throughout the basement terranes of the western U.S. There is evidence of old crust in the area from a 3.4–3.2 Ga detrital zircon population (Mueller et al., 1998, 2004) and 3.3 Ga inherited zircon (Krogh et al., 2011) from the Tobacco Root Mountains, and 2.8 Ga inherited zircon from the Highland Mountains (HM11-9) from this study. The presence of any older crust that might have existed at 2.7 Ga, however, is not indicated by the isotopic composition of these rocks, all of which are superchondritic. The isotopic signatures of the ca. 2.7 Ga crust indicate that these rocks originated from a more juvenile precursor, rather than being a product of older crust reworking.

The 2.4 Ga zircons from the two Ruby Range samples have similar, slightly subchondritic Hf isotopic signatures, with $\varepsilon_{Hf\ 2.4Ga}$ values of $-1.7 \pm 1.8$ (20-TWC-12) and $-1.6 \pm 2.5$ (20-TWC-15). On the other hand, the 2.4 Ga zircons from the Tobacco Root Mountains (20-TWC-27) and Northern Madison Range (20-TWC-26) have moderately subchondritic compositions, with $\varepsilon_{Hf\ 2.4Ga}$ values of $-6.0 \pm 1.8$ (20-TWC-27) and $-9.2 \pm 0.8$ (20-TWC-26). Our preferred interpretation of the difference in initial Hf compositions is that their parental magmas

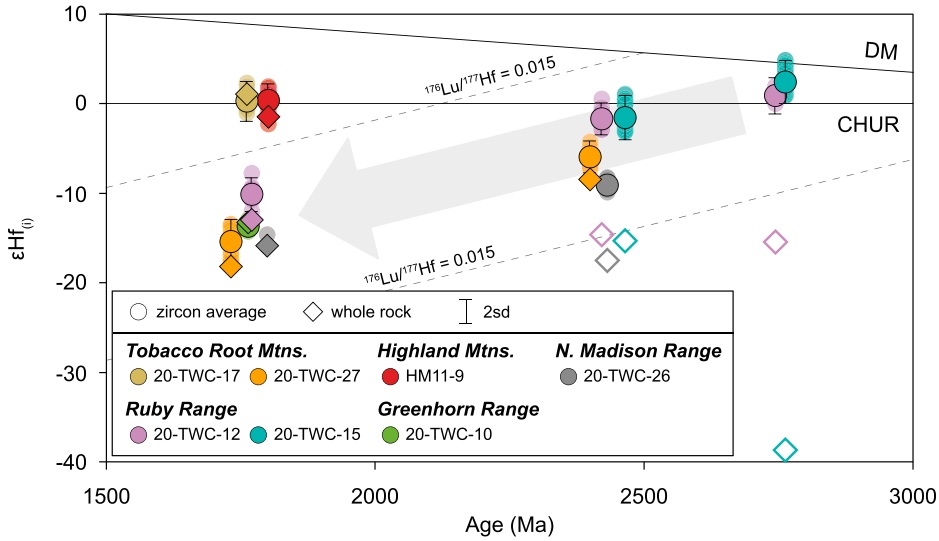


**Figure 11. Initial $\varepsilon_{Hf}$ value versus assigned U-Pb age diagram showing Hf isotopic compositions of bulk rock and zircon for seven metaigneous samples. See Table 1 for the assigned U-Pb age of each sample. Circles with solid outlines represent the mean values with uncertainty given as two standard deviations (2SD) of the population. Filled diamonds designate the bulk-rock composition that agrees with the corresponding zircon Hf composition, whereas unfilled diamonds designate the bulk-rock compositions that are decoupled from zircon. Dashed lines illustrate hypothesized Hf isotope evolutionary paths of crust with $^{176}Lu/^{177}Hf$ ratio of 0.015 (Goodge and Vervoort, 2006) that separates from the depleted mantle at different times. Arrow in the background depicts the crustal evolution from 2.7 Ga to 1.7 Ga. CHUR—chondritic uniform reservoir; DM—depleted mantle.**

assimilated various proportions of preexisting evolved crust (likely ca. 2.7 Ga). An alternative interpretation is that the 2.4 Ga zircons of the Ruby Range were formed by the reworking of ca. 2.7 Ga crust, while those of the Tobacco Root Mountains and Northern Madison Range were formed by the reworking of slightly older crust (possibly ca. 2.8 Ga in age). In either case, the 2.4 Ga zircon grains have incorporated a Neoarchean crustal component.

Evidence for 2.5–2.4 Ga magmatism has been documented in the eastern (e.g., 2.48 Ga mafic magmatism in the northern Black Hills of South Dakota, USA, Dahl et al., 2006), western (e.g., 2.45 Ga magmatism in the Farmington Canyon Complex, Mueller et al., 2011), and southern (e.g., 2.45 Ga magmatism in the Medicine Bow Mountains and Sierra Madre of southern Wyoming, Mammone et al., 2022) margins of the Wyoming Province (Fig. 1). Heaman (1997) dated the Hearst-Matachewan diabase dike swarms (Huronian Supergroup) in the southern Superior Province at 2.48–2.45 Ga. Because of the stratigraphic similarity between the Huronian Supergroup and the Snowy Pass Supergroup in the southern Wyoming Province, and the temporal correlation of ca. 2.45 Ga flood basalt volcanism between the Huronian Supergroup and the Sumi-Sariola Group in Karelia, Finland, he interpreted that this extensive Paleoproterozoic mafic magmatism may represent an ancient large igneous province that was likely related to the breakup (possibly failed) of a pre-2.5 Ga supercontinent, Kenorland. Later, Roberts et al. (2002) proposed a potential temporal connection between the cryptic ca. 2.47 Ga tectonothermal event in the Montana metasedimentary terrane region and this mafic magmatism. They argued that the tectonothermal event in the Montana metasedimentary terrane could correspond to the incipient breakup of the supercontinent Kenorland, as it coincided with the ca. 2.45 Ga mafic magmatism described by Heaman (1997). Kellogg et al. (2003), however, came to a different conclusion based on zircon U-Pb analyses of gneisses from the Beaverhead and Tendoy mountains that lie near the southwestern margin of the Montana metasedimentary terrane. They argued that the Great Falls tectonic zone, perhaps a result of subduction-related accretion between the Wyoming Province and Medicine Hat Block, can be projected through the Beaverhead-Tendoy area and postulated that the date of 2.45 Ga represents a period of contractional tectonics. Harms et al. (2004) suggest that the petrologic and structural observations of Indian Creek and the Pony–Middle Mountain metamorphic suites in the Tobacco Root Mountains indicate that the clastic sediments and igneous rocks were consolidated into a crystalline basement by burial metamorphism during the Tendoy orogeny, which would also imply the development of plate convergence and terrane collision during this period. Based on petrologic and geochronologic evidence, Harms and Baldwin (2023) further reiterate that the 2.45 Ga orogenic event, which they called the Beaverhead orogeny, reflects the presence of a convergent continental margin along the northern margin of the Montana metasedimentary terrane. Recent comprehensive paleomagnetic, geochronologic, and stratigraphic correlation studies suggest that a large igneous province was emplaced on the supercontinent Kenorland during the early Paleoproterozoic (e.g., Ernst and Bleeker, 2010; Gumsley et al., 2017). Based on this reconstruction model, the mafic dikes of the Snowy Pass Supergroup in the southern Wyoming Province have been regarded as resulting from a mantle plume. Therefore, at 2.45 Ga, the geological setting in the northern margin would seem to be different from that of the eastern and southern margins. The 2.45 Ga magmatism along the eastern and southern margins may document mafic magmatism that is associated with a mantle plume center (i.e., Matachewan plume; e.g., Ernst and Bleeker, 2010), whereas in the northern margin of the Montana metasedimentary terrane, the Wyoming Province is interpreted to have collided with one of the Rae terranes based on concurrent 2.55–2.45 Ga dates and petrologic analysis (Harms and Baldwin, 2023).

The youngest population in all of our samples is dated at 1.7 Ga, which we attribute to the Big Sky orogeny. Zircon of this age shows two distinct initial Hf isotopic components. Three samples from the Tobacco Root Mountains (20-TWC-27), Ruby Range (20-TWC-12), and Greenhorn Range (20-TWC-10) yield zircon $\varepsilon_{Hf\ 1.7Ga}$ values of $-15.5 \pm 2.5$, $-10.2 \pm 1.9$, and $-13.7 \pm 0.7$, respectively. Collectively, these are on the same broad crustal evolutionary trend as the 2.7 Ga and 2.4 Ga populations (Fig. 11). In addition, two samples from the Tobacco Root (20-TWC-17) and Highland Mountains (HM11-9) have more radiogenic zircon Hf isotopic signatures (20-TWC-17: $+ 0.3 \pm 2.2$; HM11-9: $+ 0.4 \pm 1.9$) that are approximately chondritic (Fig. 11).

The ca. 1.7 Ga time period is associated with the collision between the Wyoming Province and Medicine Hat Block (e.g., Brady et al., 2004; Harms et al., 2004). The subchondritic values of three unradiogenic samples—and the evolutionary trend from 2.7 Ga to 1.7 Ga (Fig. 11)—indicate that these rocks were predominantly reworked from preexisting crust. In contrast, the chondritic values of two other

samples infer more of a mantle-derived, juvenile input to these rocks, perhaps sourced from a less depleted mantle or a mixture of depleted mantle and older, evolved continental crust. This bimodal Hf composition further indicates that the Montana metasedimentary terrane experienced crustal reworking, accompanying the profound addition of a juvenile crustal component mixed with an older crustal component during the Wyoming–Medicine Hat incorporation.

Our time-integrated zircon Hf trajectory generally follows a crustal $^{176}Lu/^{177}Hf$ ratio of 0.015 (Goodge and Vervoort, 2006; Fig. 11) and implies that the initial formation of significant volumes of new crust occurred at ca. 2.7 Ga, and crust was subsequently reworked during the collisional processes of the Tendoy and Big Sky orogenic events. The ubiquitous 2.4 Ga and 1.7 Ga zircons with typical magmatic features in the Montana metasedimentary terrane also support the premise that the formation of new—and reworking of older—crust was an important factor leading to crustal formation and stabilization in this region.

## Zircon and Whole-Rock Hf Isotope Decoupling

In three of the samples in this study, there is significant disagreement between the zircon and bulk-rock Hf isotope values. For example, the two Ruby Range samples (20-TWC-12 and 20-TWC-15) have extremely unradiogenic bulk-rock Hf isotopic compositions when calculated at either 2.7 Ga or 2.4 Ga (20-TWC-12, $\varepsilon_{Hf\,2.75Ga} = -15.5 \pm 0.1$, $\varepsilon_{Hf\,2.42Ga} = -14.7 \pm 0.1$; 20-TWC-15, $\varepsilon_{Hf\,2.76Ga} = -38.8 \pm 0.1$, $\varepsilon_{Hf\,2.46Ga} = -15.4 \pm 0.1$) compared to the slightly super or subchondritic Hf isotopic compositions of the zircon (Table 1 and Fig. 11). The reason for this discrepancy is that for complex samples such as these, no single "assigned age" can be applied to the bulk-rock composition through time because these rocks are mixtures of components with different ages and isotopic compositions. In addition—and more significantly in some cases—the growth of garnet in these samples has resulted in the rock having a radically increased Lu/Hf ratio. The Hf evolution of the bulk rock then corresponds only up until the time when garnet altered the Lu/Hf ratio of the bulk rock; prior to that time, the calculated evolution diverges from the true path of Hf isotopic evolution of the precursor material.

Figure 12 illustrates some of the relationships between zircon and bulk-rock Hf isotopic compositions of a few samples. Panel A shows a simple case of a rock (HM11-9) with a single 1.7 Ga zircon population. The zircon and bulk-rock compositions have slightly different growth trajectories, but when calculated back to the time of zircon crystallization, both trajectories converge at the initial Hf isotopic composition of the sample at 1.7 Ga.

Panel B shows a sample (20-TWC-12) with zircon populations at 2.7 Ga, 2.4 Ga, and 1.7 Ga, each of which has a homogenous Hf isotopic composition within each population. The bulk-rock composition has a slightly superchondritic $^{176}Lu/^{177}Hf$ ratio, and when its evolutionary path is projected back in time it crosses the zircon

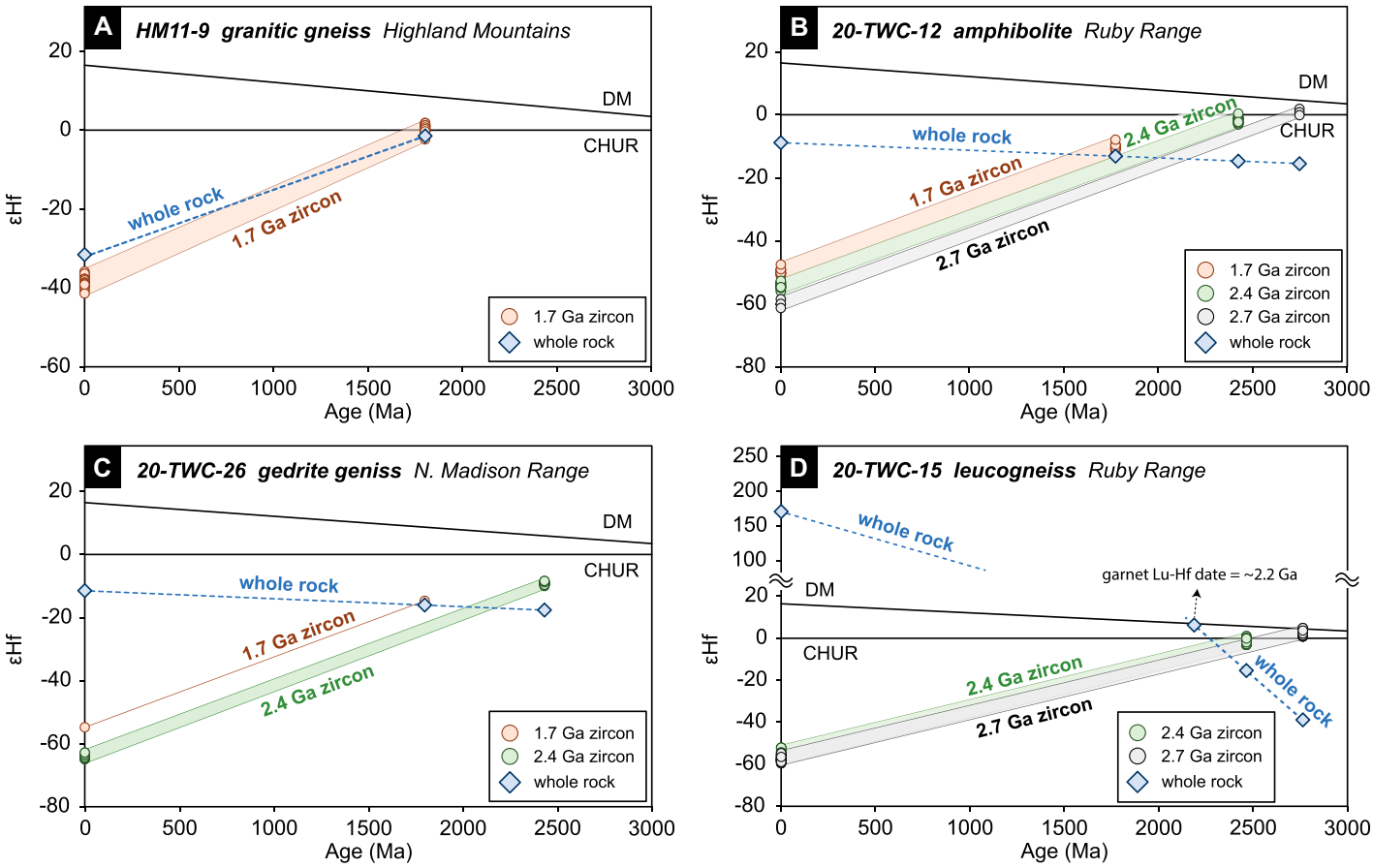


**Figure 12. Zircon and whole-rock Hf evolutionary paths from present-day to assigned zircon U-Pb ages showing coupling (e.g., HM11-9 in panel A) and decoupling (e.g., 20-TWC-12 in panel B, 20-TWC-26 in panel C, and 20-TWC-15 in panel D) zircon and whole-rock Hf isotopic compositions. Note that panel D shows two different scales in $\varepsilon_{Hf}$ axis, and the whole-rock Hf composition calculated at the garnet Lu-Hf date is also shown on the whole-rock trajectory. CHUR—chondritic uniform reservoir; DM—depleted mantle.**

growth curve at different times. At 2.7 Ga and 2.4 Ga, these apparent compositions are too unradiogenic and don't match with the composition of the zircons. The bulk rock is in better agreement with the 1.7 Ga zircon population, which indicates that this date better reflects the "age" of the bulk-rock system. In addition, 1.7 Ga represents the time of garnet growth, which results in an elevation of the Lu/Hf ratio. This higher Lu/Hf ratio does not correspond to the whole-rock evolution prior to 1.7 Ga; thus, that trajectory diverges from the zircon Hf values. A similar situation is illustrated in panel C, which shows a sample (20-TWC-26) with two zircon populations at 2.4 Ga and 1.7 Ga. The Hf isotopic composition of the bulk rock, when calculated at 2.4 Ga, is anomalously unradiogenic. It agrees reasonably well with the late Paleoproterozoic zircon, but also diverges from the zircon Hf growth trajectories prior to 1.7 Ga.

An extreme example of the different trajectories of the zircon and bulk-rock Hf isotopes is shown in panel D in relation to sample 20-TWC-15, where the bulk-rock composition has an extremely high $^{176}Lu/^{177}Hf$ ratio and a correspondingly radiogenic present-day Hf isotopic composition ($\varepsilon_{Hf(0)} = \sim+170$) due to garnet in the bulk-rock fraction. Its trajectory back in time is very steep, and the composition, calculated at both 2.7 Ga and 2.4 Ga, is far more unradiogenic than the zircon Hf composition. In this case, the steep evolutionary path of bulk rock clearly was influenced by the growth of garnet in this sample, and the Lu-Hf composition of the bulk-rock system was reset during metamorphism at ca. 2.2 Ga (T.-W. Chen, unpublished data, 2022).

In total, these data illustrate that, in complex cases like this, it is difficult to obtain meaningful initial Hf isotopic compositions from bulk-rock compositions alone, not only because these rocks may represent mixtures of different ages, but also because the Lu-Hf system was altered by the growth of new minerals (e.g., garnet) during metamorphism. These data thus illustrate, on one hand, the perils of using bulk-rock data from complex, multi-component rocks, but on the other hand the utility of integrated U-Pb age and Hf isotopes in zircon for helping to unravel these complexities.

### Comparison with Terranes in the North

For decades, numerous studies have examined the nature of basement terranes exposed in western Laurentia (see references in Fig. 10 caption), but despite this work there is still great uncertainty regarding the extent of the Wyoming Province and surrounding terranes and their spatial relationships through time. Figure 10 summarizes the zircon U-Pb dates reported from the Medicine Hat, Clearwater, and Grouse Creek blocks, as well as the Great Falls tectonic zone and Farmington zone. Even though the Montana metasedimentary terrane shares similar dates with the Medicine Hat and Clearwater blocks, as well as the Great Falls tectonic zone, the lack of isotopic data has made it difficult to correlate these separate Archean and Proterozoic terranes. To help address the question of the nature of, and relationships between, these terranes, we provide a more complete isotopic inventory of terranes in this region by using our new zircon Hf results in conjunction with previously reported Hf isotopes from the Clearwater Block (Wang et al., 2022) and with a recalculation of zircon Hf isotopic compositions from the Medicine Hat Block (Gifford et al., 2020) and Great Falls tectonic zone (Gifford et al., 2014, 2018), based on their assigned U-Pb ages. The compiled zircon Hf isotope results are given in Figure 13.

The Medicine Hat Block is an Archean terrane located between the Hearne Province and Great Falls tectonic zone (Fig. 1). Zircon U-Pb dates recovered from drill cores and xenoliths indicate that three discrete tectonomagmatic events occurred at 3.3 Ga, 2.8–2.5 Ga, and 1.8–1.7 Ga (Ross et al., 1991; Villeneuve et al., 1993; Davis et al., 1995; Gifford et al., 2020). The Paleoarchean zircons, showing an older protolith age, have negative $\varepsilon_{Hf\ 3.3Ga}$ values, which indicates the existence of Archean crust with components >3.5 Ga in the Medicine Hat Block (Gifford et al., 2020; Fig. 13). Gifford et al. (2020) proposed that the 2.8–2.5 Ga zircons record another episode of crustal formation. Unlike the Paleoarchean zircons, the 2.8–2.5 Ga zircons exhibit positive $\varepsilon_{Hf\ 2.8–2.5Ga}$ values, which indicate a much greater proportion of mantle-derived melts. In contrast, the Paleoproterozoic (1.8–1.7 Ga) zircons yield a larger range of $\varepsilon_{Hf\ 1.8–1.7Ga}$ values that are mostly highly unradiogenic, which suggests the reworking of heterogenous Archean crustal components (LaDouceur et al., 2017). Gifford et al. (2020) argued that the Medicine Hat Block and Montana metasedimentary terrane have a connection as far back as the Mesoarchean, based on the similarity of dates and isotopic compositions between these two terranes (Figs. 10 and 13). However, even though the Medicine Hat Block shares the same 2.7 Ga and 1.7 Ga age records with the Montana metasedimentary terrane, there is no evidence of 2.4 Ga magmatism from the Medicine Hat Block in the existing data. Another important orogenic event in the Montana metasedimentary terrane, the Big Sky orogeny at ca. 1.7 Ga, also has an apparently different Hf isotopic signature from that of Medicine Hat Block, based on existing data, with the Montana metasedimentary terrane showing significant involvement of juvenile mantle contributions. These differences in the 2.4 Ga and 1.7 Ga age and isotopic records do not support the model that these two terranes shared a similar history since

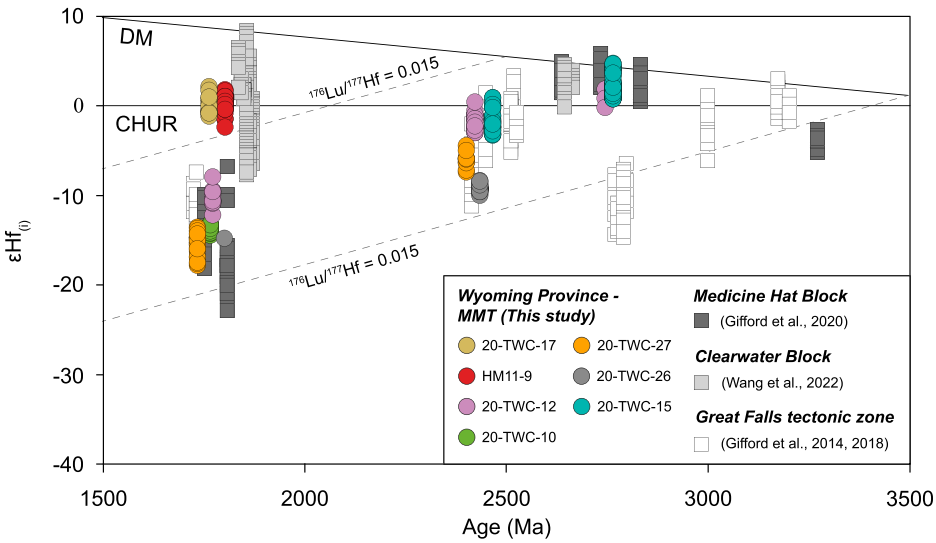


**Figure 13. Initial $\varepsilon_{Hf}$ value versus assigned U-Pb age diagram for samples from Montana metasedimentary terrane (MMT; this study), Medicine Hat Block (Gifford et al., 2020), Clearwater Block (Wang et al., 2022), and Great Falls tectonic zone (Gifford et al., 2014, 2018). $\varepsilon_{Hf(i)}$ values were calculated based on the assigned U-Pb age of each sample. Dashed lines illustrate hypothesized Hf isotope evolutionary paths of crust with $^{176}Lu/^{177}Hf$ ratio of 0.015 (Goodge and Vervoort, 2006) that separated from the depleted mantle at 2.5 Ga and 3.5 Ga. CHUR—chondritic uniform reservoir; DM—depleted mantle.**

the Mesoarchean. In addition, the Great Falls tectonic zone between the Montana metasedimentary terrane and Medicine Hat Block has been interpreted as a suture zone (O'Neill and Lopez, 1985) in response to the formation of the Little Belt arc at 1.86 Ga (Mueller et al., 2002) and closure of an oceanic basin and subduction of oceanic crust at 1.85–1.80 Ga (Bedrosian and Frost, 2022). This tectonic model, if valid, indicates that the two blocks did not incorporate until the late Paleoproterozoic.

The Clearwater Block, which is located at the western limit of Laurentia, consists of the Priest River and Clearwater complexes (Fig. 1). A zircon U-Pb date of 2651 ± 20 Ma for a gneiss indicated the presence of Archean rocks in the Priest River complex (Doughty et al., 1998). Subsequent U-Pb dating of magmatic and detrital zircon revealed several inherited and detrital dates at ca. 2.6 Ga and ca. 1.8 Ga in the Priest River complex (Doughty and Chamberlain, 2008) as well as a zircon U-Pb date of 1787 ± 2 Ma recovered from an anorthosite of the Clearwater complex (Doughty and Chamberlain, 2007). More recent zircon U-Pb studies of the Clearwater Block further confirmed two periods of crustal formation at 2.66 Ga and 1.86 Ga (Vervoort et al., 2016; Wang et al., 2022). The positive $\varepsilon_{Hf\ 2.66Ga}$ values of the Neoarchean zircons suggest that their host lavas were extracted from a juvenile, depleted mantle source. In contrast, the large range of Hf isotopes in the Paleoproterozoic zircons indicates a depleted mantle-derived magma that assimilated Neoarchean crust (Wang et al., 2022). Although both the 2.66 Ga and 1.86 Ga zircon dates of the Clearwater Block and Montana metasedimentary terrane overlap broadly (Fig. 10), their Paleoproterozoic records have different isotopic compositions, based on existing data (Fig. 13). The 1.7 Ga zircons in the Montana metasedimentary terrane exhibit bimodal Hf composition, which indicates various proportions and mixing between juvenile input and evolved crust. The Paleoproterozoic zircon population of the Montana metasedimentary terrane also extends to much less radiogenic Hf isotopic compositions. In addition, according to the distribution of basement terranes (Fig. 1), the Montana metasedimentary terrane and northern terranes, such as the Clearwater Block, have been interpreted to be separated by the Great Falls tectonic zone, a 1.8–1.7 Ga collision zone. Although it is unclear whether the Great Falls tectonic zone can be projected as far west as the Clearwater Block (e.g., Kellogg et al., 2003), the hypothesized closure of an oceanic basin and subduction of oceanic crust at 1.86–1.80 Ga (e.g., Bedrosian and Frost, 2022) would imply that the Clearwater Block and Montana metasedimentary terrane were separated terranes before late Paleoproterozoic incorporation. The 1.7 Ga, 2.4 Ga, and >2.66 Ga age peaks have not been found in the zircon U-Pb dating of magmatic bodies within the Clearwater Block (Fig. 10) despite the comprehensive sampling of previous studies (Doughty et al., 1998; Vervoort et al., 2016; Wang et al., 2022). The absence of these critical ages further suggests that the crusts of the Montana metasedimentary terrane and Clearwater Block experienced distinct Archean and Proterozoic evolutionary histories.

Within the Great Falls tectonic zone, a 1.86 Ga event was recorded in metaigneous rocks from the Little Belt and Pioneer Mountains (Fig. 1; Mueller et al., 2002; Foster et al., 2006), which has been interpreted to represent the initial timing of Wyoming Province–Medicine Hat Block collision. Mueller et al. (2002) suggested that Nd isotopic compositions from the Little Belt Mountains indicate that the 1.86 Ga gneisses were generated in a magmatic arc in response to the subduction of oceanic crust that separated the Wyoming Province from the Medicine Hat Block. The magnetotelluric data in the Wyoming Province–Great Falls tectonic zone–Medicine Hat Block region suggest that two distinct high-conductivity belts occurred along the northern and southern Great Falls tectonic zone (Bedrosian and Frost, 2022), which possibly indicates two orogenesis phases. Bedrosian and Frost (2022) proposed an evolutionary model of the Great Falls orogeny that includes an early Medicine Hat phase (Medicine Hat–Little Belt arc accretion) and a later Big Sky phase (Wyoming Province–Little Belt arc accretion). These multiple lines of evidence imply that the Wyoming Province, Great Falls tectonic zone, and Medicine Hat Block are distinct terranes. Zircon from the Little Rocky Mountains of the Great Falls tectonic zone (Fig. 1) is interpreted to show discrete pulses of crustal formation during 3.2–2.4 Ga, with a major metamorphic event at 1.8–1.7 Ga (Gifford et al., 2018). Both Archean and Paleoproterozoic zircons from the Great Falls tectonic zone have unradiogenic Hf isotopic signatures (Gifford et al., 2014, 2018; Fig. 13), which are interpreted to indicate contributions from preexisting Archean crust into the source melt. Based on the age-Hf trajectory shown in Figure 13, it appears that the Great Falls tectonic zone and Montana metasedimentary terrane have significantly different Hf evolutionary paths. The Neoarchean population of the Great Falls tectonic zone appears to be derived from the reworking of 3.2 Ga crust, in contrast to the 2.7 Ga zircon of the Montana metasedimentary terrane, which indicates derivation from juvenile mantle sources. As is true for the Medicine Hat and Clearwater blocks, the Great Falls tectonic zone lacks evidence of a strong juvenile signature at 1.7 Ga. Gifford et al. (2014, 2018) argued that the geological history of the Little Rocky Mountains in the Great Falls tectonic zone is different from that of the northern Wyoming Province and indicates more of a Medicine Hat Block affinity based on Hf-Nd isotopes. However, based on existing geochronologic and isotopic data, the Great Falls tectonic zone and the Montana metasedimentary terrane appear to represent distinct blocks with separate evolutionary histories until the late Paleoproterozoic incorporation.

The Montana metasedimentary terrane displays distinctive geochronologic and isotopic signatures that distinguish it from both the Medicine Hat and Clearwater Blocks, as well as the Great Falls tectonic zone. These signatures include a significant 2.4 Ga record and a widespread 1.7 Ga record that documents the mixing of mantle-derived magma and evolved Archean crust. We argue that the Medicine Hat Block, Clearwater Block, Great Falls tectonic zone, and Montana metasedimentary terrane have independent Archean and early Paleoproterozoic histories based on their differences in age and isotopes. Although they all exhibit varying degrees of mixing between juvenile input and evolved crust, as well as signatures of preexisting crustal reworking, the block configuration and different time-integrated Hf evolutionary paths (Fig. 13) suggest that they may not belong to a continuous basement until the late Paleoproterozoic amalgamation of western Laurentia.

## Implications for Assembly of the Supercontinent

Global zircon U-Pb date compilations have identified major age peaks during the Neoarchean (2.7–2.5 Ga) and Paleoproterozoic (2.0–1.7 Ga; e.g., Voice et al., 2011). These observations have led to speculation that the two intervals represent major periods of global crustal growth (e.g., Condie, 1998). Previous studies suggested that the episodic peaks in zircon age spectra are in response to different phases of the supercontinent cycle (e.g., Condie and Aster, 2010; Cawood et al., 2012; Hawkesworth et al., 2013). Cawood et al. (2013) proposed that these peaks reflect an interplay between increased magmatic production and the preservation potential within certain tectonic settings. Hawkesworth et al. (2009) argued that the highest potential for the preservation of continental crust is in collisional environments, and, therefore, the zircon age peaks may mark the timing of supercontinent assembly.

The Neoarchean age peak of 2.7–2.5 Ga has been identified in various cratons across the world, including the Superior Craton in North

America (e.g., Percival et al., 2001), Greenland (e.g., Thrane, 2002), the Baltic Shield in Northern Europe (e.g., Heilimo et al., 2011), the Aldan Shield in Siberia (e.g., Jahn et al., 1998), the Kaapvaal (e.g., Taylor et al., 2010) and Zimbabwe cratons (e.g., Hofmann et al., 2004) in Africa, the North China Craton in Asia (e.g., Wan et al., 2011), the Dharwar Craton in India (e.g., Lancaster et al., 2015), and the Yilgarn Craton in Australia (e.g., Griffin et al., 2004). This age is thought to have resulted from voluminous magmatic activity and corresponds to the amalgamation of supercontinent Kenorland, which is composed of the Superia, Sclavia, and Vaalbara supercratons (Bleeker, 2003). In addition, many of these Precambrian terranes also have a Paleoproterozoic tectonothermal record of 2.0–1.7 Ga, which is characterized by collisional orogenic belts such as the Taltson-Thelon belt in North America (e.g., Chacko et al., 2000), Trans-North China belt in Asia (e.g., Faure et al., 2007), and Capricorn belt in Australia (e.g., Cawood and Tyler, 2004). This age is considered to indicate the formation of another supercontinent, Nuna, which is also called the supercontinent Columbia (Zhao et al., 2002).

Zircon U-Pb dates of the Montana metasedimentary terrane also reveal populations at 2.7 Ga and 1.7 Ga. Both age records are not limited to the Montana metasedimentary terrane in western Laurentia (Fig. 10). The 2.7 Ga age coincides with the assembly of supercontinent Kenorland and has been recognized in the Beartooth-Bighorn magmatic zone and Southern accreted terrane of the Wyoming Province, as well as the Medicine Hat Block, Clearwater Block, and Great Falls tectonic zone in the north (Fig. 10). The 1.7 Ga age has been reported in the Medicine Hat Block, Clearwater Block, Great Falls tectonic zone, and Farmington zone (Fig. 10). Although this late Paleoproterozoic age has not been documented in the Beartooth-Bighorn magmatic zone and Southern accreted terrane in the Wyoming Province, it coincides with tectonism in the Trans-Hudson orogenic belt and Cheyenne belt in the eastern and southern margins of the Wyoming Province (Fig. 1), both of which are thought to represent broad suture zones (e.g., Karlstrom and Houston, 1984; Chamberlain, 1998; Corrigan et al., 2009; Kilian et al., 2016b). The contemporaneous collisional events in these areas not only mark the synchronous juxtaposition of several landmasses into western Laurentia (Mueller et al., 2005) but also fall within the time range of supercontinent Nuna assembly. Because of the age consistency, we argue that the crystalline basement complexes in western Laurentia were developed under the circumstances of global terrane amalgamation.

If this hypothesis is correct, the crustal blocks in western Laurentia amalgamated at 2.7 Ga and then again a billion years later, at 1.7 Ga. Therefore, a breakup scenario must have occurred between these two discrete episodes of block aggregation. Some previous studies argued that the event at 2.4 Ga could correspond to the initial breakup of supercontinent Kenorland (e.g., Roberts et al., 2002). However, the age and stratigraphic consistency of 2.4 Ga magmatic events among the southern Superior, Hearn, and Wyoming provinces suggest that crustal blocks located in this part of the supercontinent remained together at 2.4 Ga, and the 2.4 Ga mafic magmatism is therefore unrelated to supercontinent breakup, but rather linked to mantle plume centers (Ernst and Bleeker, 2010). The paleomagnetic and geochronologic studies of Kilian et al. (2016a, 2016b) indicate that the Wyoming Province did not separate from the southern Superior Province until at least 2.15 Ga. A recent study of volcanic and detrital zircon geochronology (Mammone et al., 2022) suggests that multiple failed rifting events occurred along the southern margins of the Superior and Wyoming provinces during the early Paleoproterozoic and eventually resulted in the ultimate separation of the Superior and Wyoming provinces at 2.07 Ga. The presence of mafic dikes in the Tobacco Root Mountains at 2.06 Ga (Mueller et al., 2004) possibly represents rifting of the northern margin of the Wyoming Province. After ~200 m.y., amalgamation of the Wyoming Province with other terranes initiated with the subduction and formation of the Little Belt arc at 1.86 Ga (Mueller et al., 2002). Incorporation of this terrane may have lasted for ~150 m.y. until 1.72 Ga (Harms et al., 2004). Subsequently, the final suturing of the Wyoming and Superior Provinces along the Trans-Hudson orogen (also the incorporation of Medicine Hat Block and Hearne Province along the Vulcan zone) occurred at 1.715 Ga (Kilian et al., 2016b), which eventually formed the Archean core of western Laurentia.

## CONCLUSIONS

The Montana metasedimentary terrane provides a window into crustal evolution in the northern Wyoming Province. Zircon U-Pb dates of seven amphibolite and orthogneiss samples that cover the region northwest of the Giletti's line reveal three discrete periods of crustal formation at 2.7 Ga, 2.4 Ga, and 1.7 Ga, which imply episodic growth of continental crust in the Montana metasedimentary terrane. The internal textures of zircons in this study are complex; some samples show no evidence of inherited cores and metamorphic overgrowths, while other samples show core-rim relationships. Based on the structures observed in cathodoluminescence (CL) images, we interpret these grains to be magmatic populations. The Neoarchean (2.7 Ga) zircon population has positive initial $\varepsilon_{Hf}$ values of +2.4 to +0.9, which represent derivation from juvenile mantle sources. The early Paleoproterozoic (2.4 Ga) zircon population has initial zircon $\varepsilon_{Hf}$ values ranging from −1.7 to −9.2, which indicates that the parental magma incorporated greater proportions of older crust. The late Paleoproterozoic (1.7 Ga) zircon population has bimodal initial Hf compositions, with a radiogenic end member ($\varepsilon_{Hf(i)} = +0.4$ to +0.3) and an unradiogenic end member ($\varepsilon_{Hf(i)} = -10.2$ to −15.5), which indicates a depleted mantle source with variable contributions from older crustal sources. In general, the isotopic signatures suggest that these samples were not produced by simple crustal reworking but were generated through the mixing of reworked crust and juvenile inputs.

The time-integrated zircon Hf trajectory generally follows the mean crustal $^{176}Lu/^{177}Hf$ ratio of 0.015, which indicates that the crust initially formed during the Neoarchean was largely reworked during the Tendoy (2.52–2.45 Ga) and Big Sky (1.78–1.72 Ga) orogenic events. The early Paleoproterozoic tectonic setting of the northern Wyoming Province appears to be different from that of its eastern and southern margins. The Montana metasedimentary terrane preserves evidence of collisional orogeny at 2.4 Ga; in contrast, the environment of the eastern and southern margins has remained tectonically stable through the emplacement of mantle plume-related dike swarms. The breakup of 2.7 Ga supercontinent Kenorland at 2.1–2.0 Ga resulted in rifting-related dike swarms in the northern and southern Wyoming Province. After ~200 m.y., the collision between the Wyoming Province and other northern terranes (e.g., Medicine Hat Block and Great Falls tectonic zone) began at ca. 1.80 Ga and culminated at ca. 1.76 Ga, resulting in the Archean core of western Laurentia.

Based on our new isotopic constraints, we propose that the Montana metasedimentary terrane in the northern Wyoming Province is isotopically distinct from the surrounding terranes in the north, such as the Medicine Hat Block, Clearwater Block, and Great Falls tectonic zone, and none of these terranes are extensions of the Montana metasedimentary terrane. In addition, the major periods of crustal formation in the Montana metasedimentary terrane are consistent with 2.7 Ga and 1.7 Ga peaks in global zircon U-Pb dates, particularly with the timing of supercontinent assembly. Therefore, we suggest that the driver of Neoarchean and late Paleoproterozoic events in the Montana metasedimentary

terrane is associated with the amalgamation of supercontinents Kenorland and Nuna.

**ACKNOWLEDGMENTS**

We thank Charles Knaack and Scott Boroughs at Washington State University for technical support in inductively coupled plasma–mass spectrometry and electron probe microanalyses. We also thank Carol Frost and Kevin Chamberlain for their thorough reviews and constructive comments. This project was supported with funding from the National Science Foundation grants EAR-1854390 to Jeffrey Vervoort and EAR-1854432 to Julia Baldwin.

**REFERENCES CITED**

Alcock, J., and Muller, P., 2012, A Paleoproterozoic sedimentary basin within the Wyoming Craton exposed in the Ruby Range: SW Montana: Identified by field relations and geochronology: Northwest Geology, v. 41, p. 47–62.

Alcock, J., Muller, P.D., and Jercinovic, M.J., 2013, Monazite ages and pressure–temperature–time paths from anatectites in the southern Ruby Range, Montana, USA: Evidence for delamination, ultramafic magmatism, and rapid uplift at ca. 1780 Ma: Canadian Journal of Earth Sciences, v. 50, no. 11, p. 1069–1084, https://doi.org/10.1139/cjes-2013-0035.

Aleinikoff, J.N., Williams, I.S., Compston, W., Stuckless, J.S., and Worl, R.G., 1989, Evidence for an Early Archean component in the Middle to Late Archean gneisses of the Wind River Range, west-central Wyoming: Conventional and ion microprobe U-Pb data: Contributions to Mineralogy and Petrology, v. 101, no. 2, p. 198–206, https://doi.org/10.1007/BF00375306.

Amelin, Y., Lee, D.-C., Halliday, A.N., and Pidgeon, R.T., 1999, Nature of the Earth's earliest crust from hafnium isotopes in single detrital zircons: Nature, v. 399, no. 6733, p. 252–255, https://doi.org/10.1038/20426.

Amelin, Y., Lee, D.-C., and Halliday, A.N., 2000, Early-middle Archaean crustal evolution deduced from Lu-Hf and U-Pb isotopic studies of single zircon grains: Geochimica et Cosmochimica Acta, v. 64, no. 24, p. 4205–4225, https://doi.org/10.1016/S0016-7037(00)00493-2.

Armstrong, R.L., Taubeneck, W.H., and Hales, P.O., 1977, Rb-Sr and K-Ar geochronometry of Mesozoic granitic rocks and their Sr isotopic composition, Oregon, Washington, and Idaho: Geological Society of America Bulletin, v. 88, p. 397–411, https://doi.org/10.1130/0016-7606(1977)88<397:RAKGOM>2.0.CO;2.

Bagdonas, D.A., Frost, C.D., and Fanning, C.M., 2016, The origin of extensive Neoarchean high-silica batholiths and the nature of intrusive complements to silicic ignimbrites: Insights from the Wyoming batholith, USA: The American Mineralogist, v. 101, no. 6, p. 1332–1347, https://doi.org/10.2138/am-2016-5512.

Bedrosian, P.A., and Frost, C.D., 2022, Geophysical extent of the Wyoming Province, western USA: Insights into ancient subduction and craton stability: Geological Society of America Bulletin, v. 135, p. 725–742, https://doi.org/10.1130/B36417.1.

Bleeker, W., 2003, The late Archean record: A puzzle in ca. 35 pieces: Lithos, v. 71, no. 2–4, p. 99–134, https://doi.org/10.1016/j.lithos.2003.07.003.

Blichert-Toft, J., 2008, The Hf isotopic composition of zircon reference material 91500: Chemical Geology, v. 253, no. 3–4, p. 252–257, https://doi.org/10.1016/j.chemgeo.2008.05.014.

Bouvier, A., Vervoort, J.D., and Patchett, P.J., 2008, The Lu–Hf and Sm–Nd isotopic composition of CHUR: Constraints from unequilibrated chondrites and implications for the bulk composition of terrestrial planets: Earth and Planetary Science Letters, v. 273, no. 1–2, p. 48–57, https://doi.org/10.1016/j.epsl.2008.06.010.

Bowers, N.E., and Chamberlain, K.R., 2006, Precambrian history of the eastern Ferris Mountains and Bear Mountain, south-central Wyoming Province: Canadian Journal of Earth Sciences, v. 43, no. 10, p. 1467–1487, https://doi.org/10.1139/e06-091.

Brady, J.B., Kovaric, D.N., Cheney, J.T., Jacob, L.J., King, J.T., Burger, H.R., and Harms, T.A., 2004, $^{40}Ar/^{39}Ar$ ages of metamorphic rocks from the Tobacco Root Mountains region, Montana, *in* Brady, J.B., Burger, H.R., Cheney, J.T., and Harms, T.A., eds., Precambrian Geology of the Tobacco Root Mountains, Montana: Geological Society of America Special Paper 377, p. 131–150, https://doi.org/10.1130/0-8137-2377-9.131.

Burger, H.R., 2004, General geology and tectonic setting of the Tobacco Root Mountains, *in* Brady, J.B., Burger, H.R., Cheney, J.T., and Harms, T.A., eds., Precambrian Geology of the Tobacco Root Mountains, Montana: Geological Society of America Special Paper 377, p. 1–14, https://doi.org/10.1130/0-8137-2377-9.1.

Cawood, P.A., and Tyler, I.M., 2004, Assembling and reactivating the Proterozoic Capricorn Orogen: Lithotectonic elements, orogenies, and significance: Precambrian Research, v. 128, no. 3–4, p. 201–218, https://doi.org/10.1016/j.precamres.2003.09.001.

Cawood, P.A., Hawkesworth, C.J., and Dhuime, B., 2012, Detrital zircon record and tectonic setting: Geology, v. 40, p. 875–878, https://doi.org/10.1130/G32945.1.

Cawood, P.A., Hawkesworth, C.J., and Dhuime, B., 2013, The continental record and the generation of continental crust: Geological Society of America Bulletin, v. 125, p. 14–32, https://doi.org/10.1130/B30722.1.

Chacko, T., De, S.K., Creaser, R.A., and Muehlenbachs, K., 2000, Tectonic setting of the Taltson magmatic zone at 1.9–2.0 Ga: A granitoid-based perspective: Canadian Journal of Earth Sciences, v. 37, no. 11, p. 1597–1609, https://doi.org/10.1139/e00-029.

Chamberlain, K.R., 1998, Medicine Bow orogeny timing of deformation and model of crustal structure produced during continent-arc collision, ca. 1.78 Ga, southeastern Wyoming: Rocky Mountain Geology, v. 33, no. 2, p. 259–277, https://doi.org/10.2113/33.2.259.

Chamberlain, K.R., and Mueller, P.A., 2007, Oldest rocks of the Wyoming Craton, *in* Van Kranendonk, M.J., Smithies, R.H., and Bennett, V.C., eds., Earth's Oldest Rocks: Elsevier, Developments in Precambrian Geology, v. 15, p. 775–791, https://doi.org/10.1016/S0166-2635(07)15063-5.

Chamberlain, K.R., and Mueller, P.A., 2019, Oldest rocks of the Wyoming Craton, *in* Van Kranendonk, M.J., Bennett, V.C., and Hoffmann, J.E., eds., Earth's Oldest Rocks (second edition): Elsevier, p. 723–739, https://doi.org/10.1016/B978-0-444-63901-1.00029-0.

Chamberlain, K.R., Frost, C.D., and Frost, B.R., 2003, Early Archean to Mesoproterozoic evolution of the Wyoming Province: Archean origins to modern lithospheric architecture: Canadian Journal of Earth Sciences, v. 40, no. 10, p. 1357–1374, https://doi.org/10.1139/e03-054.

Cheney, J.T., Alexander, A., Webb, G., Coath, C.D., McKeegan, K.D., Brady, J.B., Burger, H.R., and Harms, T.A., 2004, In situ ion microprobe $^{207}Pb/^{206}Pb$ dating of monazite from Precambrian metamorphic suites, Tobacco Root Mountains, Montana, *in* Brady, J.B., Burger, H.R., Cheney, J.T., and Harms, T.A., eds., Precambrian Geology of the Tobacco Root Mountains, Montana: Geological Society of America Special Paper 377, p. 151–180, https://doi.org/10.1130/0-8137-2377-9.151.

Chew, D.M., Petrus, J.A., and Kamber, B.S., 2014, U–Pb LA–ICPMS dating using accessory mineral standards with variable common Pb: Chemical Geology, v. 363, p. 185–199, https://doi.org/10.1016/j.chemgeo.2013.11.006.

Clowes, R.M., Burianyk, M.J.A., Gorman, A.R., and Kanasewich, E.R., 2002, Crustal velocity structure from SAREX, the southern Alberta refraction experiment: Canadian Journal of Earth Sciences, v. 39, no. 3, p. 351–373, https://doi.org/10.1139/e01-070.

Condie, K.C., 1998, Episodic continental growth and supercontinents: A mantle avalanche connection?: Earth and Planetary Science Letters, v. 163, no. 1–4, p. 97–108, https://doi.org/10.1016/S0012-821X(98)00178-2.

Condie, K.C., and Aster, R.C., 2010, Episodic zircon age spectra of orogenic granitoids: The supercontinent connection and continental growth: Precambrian Research, v. 180, no. 3–4, p. 227–236, https://doi.org/10.1016/j.precamres.2010.03.008.

Corfu, F., 1993, The evolution of the southern Abitibi greenstone belt in light of precise U-Pb geochronology: Economic Geology, v. 88, no. 6, p. 1323–1340, https://doi.org/10.2113/gsecongeo.88.6.1323.

Corfu, F., Hanchar, J.M., Hoskin, P.W.O., and Kinny, P., 2003, Atlas of zircon textures: Reviews in Mineralogy and Geochemistry, v. 53, no. 1, p. 469–500, https://doi.org/10.2113/0530469.

Corrigan, D., Pehrsson, S., Wodicka, N., and De Kemp, E., 2009, The Palaeoproterozoic Trans-Hudson Orogen: A prototype of modern accretionary processes, *in* Murphy, J.B., Keppie, J.D., and Hynes, A.J., eds., Ancient Orogens and Modern Analogues: Geological Society, London, Special Publication 327, p. 457–479, https://doi.org/10.1144/SP327.19.

Cox, D.M., Frost, C.D., and Chamberlain, K.R., 2000, 2.01-Ga Kennedy dike swarm, southeastern Wyoming: Record of a rifted margin along the southern Wyoming province: Rocky Mountain Geology, v. 35, no. 1, p. 7–30, https://doi.org/10.2113/35.1.7.

Cramer, M., 2015, Proterozoic tectonometamorphic evolution of the Ruby Range, SW Montana, USA: Insights from phase equilibria modeling and in situ monazite petrochronology [M.Sc. thesis]: Missoula, Montana, University of Montana, 128 p.

Dahl, P.S., Holm, D.K., Gardner, E.T., Hubacher, F.A., and Foland, K.A., 1999, New constraints on the timing of early Proterozoic tectonism in the Black Hills (South Dakota), with implications for docking of the Wyoming province with Laurentia: Geological Society of America Bulletin, v. 111, p. 1335–1349, https://doi.org/10.1130/0016-7606(1999)111<1335:NCOTTO>2.3.CO;2.

Dahl, P.S., Hamilton, M.A., Terry, M.P., Roberts, H.J., Kelly, S.P., Frei, R., Jercinovic, M.J., and Williams, M.L., 2002, Comparative ion and electron microprobe dating of Wyoming province monazite, with tectonic and analytical implications: Geological Society of America Abstracts with Programs, v. 34, no. 1, p. A9.

Dahl, P.S., Hamilton, M.A., Wooden, J.L., Foland, K.A., Frei, R., McCombs, J.A., and Holm, D.K., 2006, 2480 Ma mafic magmatism in the northern Black Hills, South Dakota: A new link connecting the Wyoming and Superior cratons: Canadian Journal of Earth Sciences, v. 43, no. 10, p. 1579–1600, https://doi.org/10.1139/e06-066.

Davis, W.J., Berman, R., Kjarsgaard, B., and Ross, G.M., 1995, U–Pb geochronology and isotopic studies of crustal xenoliths from the Archean Medicine Hat block, northern Montana and southern Alberta: Paleoproterozoic reworking of Archean crust, Alberta Basement Transects Workshop: Lithoprobe 1995, v. 47, p. 330–335.

DePaolo, D.J., and Wasserburg, G.J., 1976, Nd isotopic variations and petrogenetic models: Geophysical Research Letters, v. 3, no. 5, p. 249–252, https://doi.org/10.1029/GL003i005p00249.

Doughty, P.T., and Chamberlain, K.R., 2007, Age of Paleoproterozoic basement and related rocks in the Clearwater complex, northern Idaho, USA, *in* Link, P.K., and Lewis, R.S., eds., Proterozoic Geology of Western North America and Siberia: Society for Sedimentary Geology (SEPM) Special Publication 86, p. 9–35, https://doi.org/10.2110/pec.07.86.0009.

Doughty, P.T., and Chamberlain, K.R., 2008, Protolith age and timing of Precambrian magmatic and metamorphic events in the Priest River complex, northern Rockies: Canadian Journal of Earth Sciences, v. 45, no. 1, p. 99–116, https://doi.org/10.1139/e07-067.

Doughty, P.T., Price, R.A., and Parrish, R.R., 1998, Geology and U-Pb geochronology of Archean basement and Proterozoic cover in the Priest River complex, northwestern United States, and their implications for Cordilleran structure and Precambrian continent reconstructions: Canadian Journal of Earth Sciences, v. 35, no. 1, p. 39–54, https://doi.org/10.1139/e97-083.

Egger, A.E., Dumitru, T.A., Miller, E.L., Savage, C.F.I., and Wooden, J.L., 2003, Timing and nature of Tertiary plutonism and extension in the Grouse Creek Mountains, Utah: International Geology Review, v. 45, no. 6, p. 497–532, https://doi.org/10.2747/0020-6814.45.6.497.

Ernst, R., and Bleeker, W., 2010, Large igneous provinces (LIPs), giant dyke swarms, and mantle plumes: Significance for breakup events within Canada and adjacent regions from 2.5 Ga to the Present: Canadian Journal of Earth Sciences, v. 47, no. 5, p. 695–739, https://doi.org/10.1139/E10-025.

Erslev, E.A., and Sutter, J.F., 1990, Evidence for Proterozoic mylonitization in the northwestern Wyoming province: Geological Society of America Bulletin, v. 102, p. 1681–1694, https://doi.org/10.1130/0016-7606(1990)102<1681:EFPMIT>2.3.CO;2.

Faure, M., Trap, P., Lin, W., Monié, P., and Bruguier, O., 2007, Polyorogenic evolution of the Paleoproterozoic Trans-North China belt—New insights from the Lüliangshan-Hengshan-Wutaishan and Fuping massifs: Episodes: Journal of International Geoscience, v. 30, no. 2, p. 96–107, https://doi.org/10.18814/epiiugs/2007/v30i2/004.

Fisher, C.M., and Vervoort, J.D., 2018, Using the magmatic record to constrain the growth of continental crust—The Eoarchean zircon Hf record of Greenland: Earth and Planetary Science Letters, v. 488, p. 79–91, https://doi.org/10.1016/j.epsl.2018.01.031.

Fisher, C.M., Hanchar, J.M., Samson, S.D., Dhuime, B., Blichert-Toft, J., Vervoort, J.D., and Lam, R., 2011, Synthetic zircon doped with hafnium and rare earth elements: A reference material for in situ hafnium isotope analysis: Chemical Geology, v. 286, no. 1–2, p. 32–47, https://doi.org/10.1016/j.chemgeo.2011.04.013.

Fisher, C.M., Vervoort, J.D., and DuFrane, S.A., 2014, Accurate Hf isotope determinations of complex zircons using the "laser ablation split stream" method: Geochemistry, Geophysics, Geosystems, v. 15, no. 1, p. 121–139, https://doi.org/10.1002/2013GC004962.

Fisher, L.B., and Stacey, J.S., 1986, For the Archean gneisses of the Granite Mountains, Wyoming: Shorter contributions to isotope research: Topical Reports on Geochronology and Isotope Geochemistry 1622, p. 13.

Foster, D.A., Mueller, P.A., Mogk, D.W., Wooden, J.L., and Vogl, J.J., 2006, Proterozoic evolution of the western margin of the Wyoming Craton: Implications for the tectonic and magmatic evolution of the northern Rocky Mountains: Canadian Journal of Earth Sciences, v. 43, no. 10, p. 1601–1619, https://doi.org/10.1139/e06-052.

Frost, C.D., and Fanning, C.M., 2006, Archean geochronological framework of the Bighorn Mountains, Wyoming: Canadian Journal of Earth Sciences, v. 43, no. 10, p. 1399–1418, https://doi.org/10.1139/e06-051.

Frost, C.D., Frost, B.R., Chamberlain, K.R., and Hulsebosch, T.P., 1998, The Late Archean history of the Wyoming province as recorded by granitic magmatism in the Wind River Range, Wyoming: Precambrian Research, v. 89, no. 3–4, p. 145–173, https://doi.org/10.1016/S0301-9268(97)00082-X.

Frost, C.D., Fruchey, B.L., Chamberlain, K.R., and Ronald Frost, B., 2006, Archean crustal growth by lateral accretion of juvenile supracrustal belts in the south-central Wyoming Province: Canadian Journal of Earth Sciences, v. 43, no. 10, p. 1533–1555, https://doi.org/10.1139/e06-092.

Frost, C.D., Swapp, S.M., Frost, B.R., Finley-Blasi, L., and Fitz-Gerald, D.B., 2016, Leucogranites of the Teton Range, Wyoming: A record of Archean collisional orogeny: Geochimica et Cosmochimica Acta, v. 185, p. 528–549, https://doi.org/10.1016/j.gca.2015.12.015.

Frost, C.D., McLaughlin, J.F., Frost, B.R., Fanning, C.M., Swapp, S.M., Kruckenberg, S.C., and Gonzalez, J., 2017, Hadean origins of Paleoarchean continental crust in the central Wyoming Province: Geological Society of America Bulletin, v. 129, p. 259–280, https://doi.org/10.1130/B31555.1.

Gerwin, D., 2006, A regional study of pressures, temperatures, and ages of metamorphosed pelitic rocks in southwestern Montana [B.A. thesis]: Northampton, Massachussetts, Smith College, 80 p.

Gifford, J.N., Mueller, P.A., Foster, D.A., and Mogk, D.W., 2014, Precambrian crustal evolution in the Great Falls tectonic zone: Insights from xenoliths from the Montana Alkali Province: The Journal of Geology, v. 122, no. 5, p. 531–548, https://doi.org/10.1086/677262.

Gifford, J.N., Mueller, P.A., Foster, D.A., and Mogk, D.W., 2018, Extending the realm of Archean crust in the Great Falls tectonic zone: Evidence from the Little Rocky Mountains, Montana: Precambrian Research, v. 315, p. 264–281, https://doi.org/10.1016/j.precamres.2018.07.021.

Gifford, J.N., Malone, S.J., and Mueller, P.A., 2020, The Medicine Hat Block and the early Paleoproterozoic assembly of western Laurentia: Geosciences, v. 10, no. 7, https://doi.org/10.3390/geosciences10070271.

Giletti, B.J., 1966, Isotopic ages from southwestern Montana: Journal of Geophysical Research, v. 71, no. 16, p. 4029–4036, https://doi.org/10.1029/JZ071i016p04029.

Goodge, J.W., and Vervoort, J.D., 2006, Origin of Mesoproterozoic A-type granites in Laurentia: Hf isotope evidence: Earth and Planetary Science Letters, v. 243, no. 3–4, p. 711–731, https://doi.org/10.1016/j.epsl.2006.01.040.

Gorman, A.R., Clowes, R.M., Ellis, R.M., Henstock, T.J., Levander, A., Spence, G.D., Keller, G.R., Miller, K.C., Snelson, C.M., and Burianyk, M.J.A., 2002, Deep Probe: Imaging the roots of western North America: Canadian Journal of Earth Sciences, v. 39, no. 3, p. 375–398, https://doi.org/10.1139/e01-064.

Grace, R.L.B., Chamberlain, K.R., Frost, B.R., and Frost, C.D., 2006, Tectonic histories of the Paleo- to Mesoarchean Sacawee block and Neoarchean Oregon Trail structural belt of the south-central Wyoming Province: Canadian Journal of Earth Sciences, v. 43, no. 10, p. 1445–1466, https://doi.org/10.1139/e06-083.

Griffin, W.L., Belousova, E.A., Shee, S.R., Pearson, N.J., and O'Reilly, S.Y., 2004, Archean crustal evolution in the northern Yilgarn Craton: U–Pb and Hf-isotope evidence from detrital zircons: Precambrian Research, v. 131, no. 3–4, p. 231–282, https://doi.org/10.1016/j.precamres.2003.12.011.

Gumsley, A.P., Chamberlain, K.R., Bleeker, W., Söderlund, U., De Kock, M.O., Larsson, E.R., and Bekker, A., 2017, Timing and tempo of the Great Oxidation Event: Proceedings of the National Academy of Sciences of the United States of America, v. 114, no. 8, p. 1811–1816, https://doi.org/10.1073/pnas.1608824114.

Harlan, S.S., Geissman, J.W., Snee, L.W., and Reynolds, R.L., 1996, Late Cretaceous remagnetization of Proterozoic mafic dikes, southern Highland Mountains, southwestern Montana: A paleomagnetic and $^{40}Ar/^{39}Ar$ study: Geological Society of America Bulletin, v. 108, p. 653–668, https://doi.org/10.1130/0016-7606(1996)108<0653:LCROPM>2.3.CO;2.

Harlan, S.S., Geissman, J.W., and Premo, W.R., 2003, Paleomagnetism and geochronology of an early Proterozoic quartz diorite in the southern Rind River Range, Wyoming, USA: Tectonophysics, v. 362, no. 1–4, p. 105–122, https://doi.org/10.1016/S0040-1951(02)00633-9.

Harms, T.A., and Baldwin, J.A., 2023, Paleoproterozoic geology of SW Montana: Implications for the paleogeography of the Wyoming Craton and for the consolidation of Laurentia, *in* Whitmeyer, S.J., Williams, M.L., Kellett, D.A., and Tikoff, B., eds., Laurentia: Turning Points in the Evolution of a Continent: Geological Society of America Memoir 220, p. 65–79, https://doi.org/10.1130/2022.1220(05).

Harms, T.A., Brady, J.B., Burger, H.R., and Cheney, J.T., 2004, Advances in the geology of the Tobacco Root Mountains, Montana, and their implications for the history of the northern Wyoming province, *in* Brady, J.B., Burger, H.R., Cheney, J.T., and Harms, T.A., Precambrian Geology of the Tobacco Root Mountains, Montana: Geological Society of America Special Paper 377, p. 227–243, https://doi.org/10.1130/0-8137-2377-9.227.

Hawkesworth, C., Cawood, P., Kemp, T., Storey, C., and Dhuime, B., 2009, A matter of preservation: Science, v. 323, no. 5910, p. 49–50, https://doi.org/10.1126/science.1168549.

Hawkesworth, C., Cawood, P., and Dhuime, B., 2013, Continental growth and the crustal record: Tectonophysics, v. 609, p. 651–660, https://doi.org/10.1016/j.tecto.2013.08.013.

Heaman, L.M., 1997, Global mafic magmatism at 2.45 Ga: Remnants of an ancient large igneous province?: Geology, v. 25, p. 299–302, https://doi.org/10.1130/0091-7613(1997)025<0299:GMMAGR>2.3.CO;2.

Heilimo, E., Halla, J., and Huhma, H., 2011, Single-grain zircon U–Pb age constraints of the western and eastern sanukitoid zones in the Finnish part of the Karelian Province: Lithos, v. 121, no. 1–4, p. 87–99, https://doi.org/10.1016/j.lithos.2010.10.006.

Henstock, T.J., Levander, A., Snelson, C.M., Keller, G.R., Miller, K.C., Harder, S.H., Gorman, A.R., Clowes, R.M., Burianyk, M.J.A., and Humphreys, E.D., 1998, Probing the Archean and Proterozoic lithosphere of western North America: GSA Today, v. 8, no. 7, p. 1–5.

Hiess, J., Condon, D.J., McLean, N., and Noble, S.R., 2012, $^{238}U/^{235}U$ systematics in terrestrial uranium-bearing minerals: Science, v. 335, no. 6076, p. 1610–1614, https://doi.org/10.1126/science.1215507.

Hofmann, A., Dirks, P.H.G.M., and Jelsma, H.A., 2004, Clastic sedimentation in a Late Archaean accretionary terrain, Midlands greenstone belt, Zimbabwe: Precambrian Research, v. 129, no. 1–2, p. 47–69, https://doi.org/10.1016/j.precamres.2003.09.017.

Isakson, V.H., 2012, Constraining the origin and evolution of the basement rocks in the Raft River, Albion, Grouse Creek Core Complex, northwestern Utah and southern Idaho [M.Sc. thesis]: Pullman, Washington, Washington State University, 82 p.

Jackson, S.E., Pearson, N.J., Griffin, W.L., and Belousova, E.A., 2004, The application of laser ablation-inductively coupled plasma-mass spectrometry to in situ U–Pb zircon geochronology: Chemical Geology, v. 211, no. 1–2, p. 47–69, https://doi.org/10.1016/j.chemgeo.2004.06.017.

Jaffey, A.H., Flynn, K.F., Glendenin, L.E., Bentley, W.C., and Essling, A.M., 1971, Precision measurement of half-lives and specific activities of $^{235}U$ and $^{238}U$: Physical Review C, v. 4, no. 5, p. 1889–1906, https://doi.org/10.1103/PhysRevC.4.1889.

Jahn, B.-M., Gruau, G., Capdevila, R., Cornichet, J., Nemchin, A., Pidgeon, R., and Rudnik, V.A., 1998, Archean crustal evolution of the Aldan Shield, Siberia: Geochemical and isotopic constraints: Precambrian Research, v. 91, no. 3–4, p. 333–363, https://doi.org/10.1016/S0301-9268(98)00057-6.

James, H.L., and Hedge, C.E., 1980, Age of the basement rocks of southwest Montana: Geological Society of America Bulletin, v. 91, p. 11–15, https://doi.org/10.1130/0016-7606(1980)91<11:AOTBRO>2.0.CO;2.

Johnson, T.A., Vervoort, J.D., Ramsey, M.J., Aleinikoff, J.N., and Southworth, S., 2018, Constraints on the timing and duration of orogenic events by combined Lu–Hf and Sm–Nd geochronology: An example from the Grenville orogeny: Earth and Planetary Science Letters, v. 501, p. 152–164, https://doi.org/10.1016/j.epsl.2018.08.030.

Jones, C.L., 2008, U-Pb geochronology of monazite and zircon in Precambrian metamorphic rocks from the Ruby Range, SW Montana: Deciphering geological events that shaped the NW Wyoming province [M.Sc. thesis]: Kent, Ohio, Kent State University, 119 p.

Karlstrom, K.E., and Houston, R.S., 1984, The Cheyenne belt: Analysis of a Proterozoic suture in southern Wyoming: Precambrian Research, v. 25, no. 4, p. 415–446, https://doi.org/10.1016/0301-9268(84)90012-3.

Kellogg, K.S., Snee, L.W., and Unruh, D.M., 2003, The Mesoproterozoic Beaverhead impact structure and its tectonic setting, Montana-Idaho: $^{40}Ar/^{39}Ar$ and U-Pb isotopic constraints: The Journal of Geology, v. 111, no. 6, p. 639–652, https://doi.org/10.1086/378339.

Kilian, T.M., Bleeker, W., Chamberlain, K., Evans, D.A.D., and Cousens, B., 2016a, Palaeomagnetism, geochronology and geochemistry of the Palaeoproterozoic Rabbit Creek and Powder River dyke swarms: Implications for Wyoming in supercraton Superia: Geological Society, London, Special Publication 424, p. 15–45, https://doi.org/10.1144/SP424.7.

Kilian, T.M., Chamberlain, K.R., Evans, D.A.D., Bleeker, W., and Cousens, B.L., 2016b, Wyoming on the run—Toward final Paleoproterozoic assembly of Laurentia: Geology, v. 44, p. 863–866, https://doi.org/10.1130/G38042.1.

Krogh, T.E., Kamo, S.L., Hanley, T.B., Hess, D.F., Dahl, P.S., and Johnson, R.E., 2011, Geochronology and geochemistry of Precambrian gneisses, metabasites, and pegmatite from the Tobacco Root Mountains, northwestern

Wyoming Craton, Montana: Canadian Journal of Earth Sciences, v. 48, no. 2, p. 161–185, https://doi.org/10.1139/E10-095.

LaDouceur, B.O., Gifford, J., Malone, S., and Davis, B., 2017, The significance of the Medicine Hat Block (southern Alberta, northern Montana) in the assembly of Laurentia: New interpretations from recent single grain zircon geochronological and geochemical data: AGU Fall Meeting Abstracts, v. 2017, abstract #T11C-0473.

Lancaster, P.J., Dey, S., Storey, C.D., Mitra, A., and Bhunia, R.K., 2015, Contrasting crustal evolution processes in the Dharwar Craton: Insights from detrital zircon U–Pb and Hf isotopes: Gondwana Research, v. 28, no. 4, p. 1361–1372, https://doi.org/10.1016/j.gr.2014.10.010.

Ludwig, K.R., 1998, On the treatment of concordant uranium-lead ages: Geochimica et Cosmochimica Acta, v. 62, no. 4, p. 665–676, https://doi.org/10.1016/S0016-7037(98)00059-3.

Ludwig, K.R., and Stuckless, J.S., 1978, Uranium-lead isotope systematics and apparent ages of zircons and other minerals in Precambrian granitic rocks, Granite Mountains, Wyoming: Contributions to Mineralogy and Petrology, v. 65, no. 3, p. 243–254, https://doi.org/10.1007/BF00375510.

Mammone, N., Bekker, A., Chamberlain, K., and Kuznetsov, A.B., 2022, Testing the early Paleoproterozoic connection of the Superior and Wyoming cratons with geochronology and geochemistry: Precambrian Research, v. 381, https://doi.org/10.1016/j.precamres.2022.106818.

Matthews, J.A., 2006, Metamorphism of Precambrian rocks in the southern Highland Mountains, southwestern Montana, *in* Annual Keck Symposium in Geology Proceedings, v. 19, p. 213–217.

Mogk, D.W., Mueller, P.A., and Wooden, J.L., 1988, Archean tectonics of the north Snowy block, Beartooth Mountains, Montana: The Journal of Geology, v. 96, no. 2, p. 125–141, https://doi.org/10.1086/629205.

Mogk, D.W., Mueller, P.A., and Wooden, J.L., 1992, The nature of Archean terrane boundaries: An example from the northern Wyoming Province: Precambrian Research, v. 55, no. 1–4, p. 155–168, https://doi.org/10.1016/0301-9268(92)90020-O.

Mogk, D.W., Burger, H.R., Mueller, P.A., D'Arcy, K., Heatherington, A.L., Wooden, J.L., Abeyta, R.L., Martin, J., and Jacob, L.J., 2004, Geochemistry of quartzofeldspathic gneisses and metamorphic mafic rocks of the Indian Creek and Pony–Middle Mountain metamorphic suites, Tobacco Root Mountains, Montana *in* Brady, J.B., Burger, H.R., Cheney, J.T., and Harms, T.A., eds., Precambrian Geology of the Tobacco Root Mountains: Geological Society of America Special Paper 377, p. 15–46, https://doi.org/10.1130/0-8137-2377-9.15.

Mogk, D.W., Frost, C.D., Mueller, P.A., Frost, B.R., and Henry, D.J., 2023, Crustal genesis and evolution of the Archean Wyoming Province: Continental growth through vertical magmatic and horizontal tectonic processes, *in* Whitmeyer, S.J., Williams, M.L., Kellett, D.A., and Tikoff, B., eds., Laurentia: Turning Points in the Evolution of a Continent: Geological Society of America Memoir 220, p. 1–24, https://doi.org/10.1130/2022.1220(01).

Morel, M.L.A., Nebel, O., Nebel-Jacobsen, Y.J., Miller, J.S., and Vroon, P.Z., 2008, Hafnium isotope characterization of the GJ-1 zircon reference material by solution and laser-ablation MC-ICPMS: Chemical Geology, v. 255, no. 1–2, p. 231–235, https://doi.org/10.1016/j.chemgeo.2008.06.040.

Mueller, P., Mogk, D.W., and Wooden, J.L., 2012, Age and composition of crystalline basement in the Armstead anticline, southwestern Montana: Northwest Geology, v. 41, p. 63–70.

Mueller, P.A., and Frost, C.D., 2006, The Wyoming Province: A distinctive Archean craton in Laurentian North America: Canadian Journal of Earth Sciences, v. 43, no. 10, p. 1391–1397, https://doi.org/10.1139/e06-075.

Mueller, P.A., Shuster, R.D., Graves, M.A., Wooden, J.L., Bowes, D.R., Lewis, S., and Berg, R.B., 1988, Age and composition of a late Archean magmatic complex, Beartooth Mountains, Montana–Wyoming: Montana Bureau of Mines and Geology, v. 96, p. 7–22.

Mueller, P.A., Wooden, J.L., and Nutman, A.P., 1992, 3.96 Ga zircons from an Archean quartzite, Beartooth Mountains, Montana: Geology, v. 20, p. 327–330, https://doi.org/10.1130/0091-7613(1992)020<0327:GZFAAQ>2.3.CO;2.

Mueller, P.A., Shuster, R.D., Wooden, J.L., Erslev, E.A., and Bowes, D.R., 1993, Age and composition of Archean crystalline rocks from the southern Madison Range, Montana: Implications for crustal evolution in the Wyoming Craton: Geological Society of America Bulletin, v. 105, p. 437–446, https://doi.org/10.1130/0016-7606(1993)105<0437:AACOAC>2.3.CO;2.

Mueller, P.A., Wooden, J.L., Mogk, D.W., Nutman, A.P., and Williams, I.S., 1996, Extended history of a 3.5 Ga trondhjemitic gneiss, Wyoming Province, USA: Evidence from U–Pb systematics in zircon: Precambrian Research, v. 78, no. 1–3, p. 41–52, https://doi.org/10.1016/0301-9268(95)00067-4.

Mueller, P.A., Wooden, J.L., Nutman, A.P., and Mogk, D.W., 1998, Early Archean crust in the northern Wyoming province: Evidence from U–Pb ages of detrital zircons: Precambrian Research, v. 91, no. 3–4, p. 295–307, https://doi.org/10.1016/S0301-9268(98)00055-2.

Mueller, P.A., Heatherington, A.L., Kelly, D.M., Wooden, J.L., and Mogk, D.W., 2002, Paleoproterozoic crust within the Great Falls tectonic zone: Implications for the assembly of southern Laurentia: Geology, v. 30, p. 127–130, https://doi.org/10.1130/0091-7613(2002)030<0127:PCWTGF>2.0.CO;2.

Mueller, P.A., Burger, H.R., Wooden, J.L., Heatherington, A.L., Mogk, D.W.D., Arcy, K., Brady, J.B., Cheney, J.T., and Harms, T.A., 2004, Age and evolution of the Precambrian crust of the Tobacco Root Mountains, Montana, *in* Brady, J.B., Burger, H.R., Cheney, J.T., and Harms, T.A., eds., Precambrian Geology of the Tobacco Root Mountains, Montana: Geological Society of America Special Paper 377, p. 181–202, https://doi.org/10.1130/0-8137-2377-9.181.

Mueller, P.A., Burger, H.R., Wooden, J.L., Brady, J.B., Cheney, J.T., Harms, T.A., Heatherington, A.L., and Mogk, D.W., 2005, Paleoproterozoic metamorphism in the northern Wyoming province: Implications for the assembly of Laurentia: The Journal of Geology, v. 113, no. 2, p. 169–179, https://doi.org/10.1086/427667.

Mueller, P.A., Wooden, J.L., Mogk, D.W., Henry, D.J., and Bowes, D.R., 2010, Rapid growth of an Archean continent by arc magmatism: Precambrian Research, v. 183, no. 1, p. 70–88, https://doi.org/10.1016/j.precamres.2010.07.013.

Mueller, P.A., Wooden, J.L., Mogk, D.W., and Foster, D.A., 2011, Paleoproterozoic evolution of the Farmington zone: Implications for terrane accretion in southwestern Laurentia: Lithosphere, v. 3, no. 6, p. 401–408, https://doi.org/10.1130/L161.1.

Mueller, P.A., Mogk, D.W., Henry, D.J., Wooden, J.L., and Foster, D.A., 2014, The plume to plate transition: Hadean and Archean crustal evolution in the northern Wyoming Province, USA, *in* Dilek, Y, and Furnes, H., eds., Evolution of Archean Crust and Early Life: Springer, p. 23–54.

Naylor, R., Steiger, R., and Wasserburg, G., 1970, U-Th-Pb and Rb-Sr systematics in 2700 × $10^6$-year old plutons from the southern Wind River Range, Wyoming: Geochimica et Cosmochimica Acta, v. 34, no. 11, p. 1133–1159, https://doi.org/10.1016/0016-7037(70)90055-4.

O'Neill, J.M., and Lopez, D.A., 1985, Character and regional significance of Great Falls tectonic zone, east-central Idaho and west-central Montana: American Association of Petroleum Geologists Bulletin, v. 69, no. 3, p. 437–447.

O'Neill, J.M., Duncan, M.S., and Zartman, R.E., 1988, An early Proterozoic gneiss dome in the Highland Mountains, southwestern Montana: Montana Bureau of Mines and Geology Open File Report 247, 81 p.

Paces, J.B., and Miller, J.D., Jr., 1993, Precise U-Pb ages of Duluth complex and related mafic intrusions, northeastern Minnesota: Geochronological insights to physical, petrogenetic, paleomagnetic, and tectonomagmatic processes associated with the 1.1 Ga midcontinent rift system: Journal of Geophysical Research: Solid Earth, v. 98, no. B8, p. 13,997–14,013, https://doi.org/10.1029/93JB01159.

Patchett, P.J., 1983, Importance of the Lu-Hf isotopic system in studies of planetary chronology and chemical evolution: Geochimica et Cosmochimica Acta, v. 47, no. 1, p. 81–91, https://doi.org/10.1016/0016-7037(83)90092-3.

Patchett, P.J., and Tatsumoto, M., 1980, Hafnium isotope variations in oceanic basalts: Geophysical Research Letters, v. 7, no. 12, p. 1077–1080, https://doi.org/10.1029/GL007i012p01077.

Paton, C., Woodhead, J.D., Hellstrom, J.C., Hergt, J.M., Greig, A., and Maas, R., 2010, Improved laser ablation U-Pb zircon geochronology through robust downhole fractionation correction: Geochemistry, Geophysics, Geosystems, v. 11, no. 3, https://doi.org/10.1029/2009GC002618.

Percival, J.A., Stern, R.A., and Skulski, T., 2001, Crustal growth through successive arc magmatism: Reconnaissance U–Pb SHRIMP data from the northeastern Superior Province, Canada: Precambrian Research, v. 109, no. 3–4, p. 203–238, https://doi.org/10.1016/S0301-9268(01)00148-6.

Premo, W.R., and Van Schmus, W.R., 1989, Zircon geochronology of Precambrian rocks in southeastern Wyoming and northern Colorado: Proterozoic geology of the southern Rocky Mountains, *in* Grambling, J.A., and Tewksbury, B.J., Proterozoic Geology of the Southern Rocky Mountains: Geological Society of America Special Paper 235, p. 13–32, https://doi.org/10.1130/SPE235-p13.

Premo, W.R., Helz, R.T., Zientek, M.L., and Langston, R.B., 1990, U-Pb and Sm-Nd ages for the Stillwater Complex and its associated sills and dikes, Beartooth Mountains, Montana: Identification of a parent magma?: Geology, v. 18, p. 1065–1068, https://doi.org/10.1130/0091-7613(1990)018<1065:UPASNA>2.3.CO;2.

Roberts, H., Dahl, P., Kelley, S., and Frei, R., 2002, New $^{207}Pb$–$^{206}Pb$ and $^{40}Ar$–$^{39}Ar$ ages from SW Montana, USA: Constraints on the Proterozoic and Archaean tectonic and depositional history of the Wyoming Province: Precambrian Research, v. 117, no. 1–2, p. 119–143, https://doi.org/10.1016/S0301-9268(02)00076-1.

Ross, G.M., Parrish, R.R., Villeneuve, M.E., and Bowring, S.A., 1991, Geophysics and geochronology of the crystalline basement of the Alberta Basin, western Canada: Canadian Journal of Earth Sciences, v. 28, no. 4, p. 512–522, https://doi.org/10.1139/e91-045.

Rubatto, D., 2017, Zircon: The metamorphic mineral: Reviews in Mineralogy and Geochemistry, v. 83, no. 1, p. 261–295, https://doi.org/10.2138/rmg.2017.83.9.

Sims, P.K., O'Neill, J.M., Bankey, V., and Anderson, E., 2004, Precambrian basement geologic map of Montana—An interpretation of aeromagnetic anomalies: U.S. Geological Survey Scientific Investigations Map 2829.

Sláma, J., Košler, J., Condon, D.J., Crowley, J.L., Gerdes, A., Hanchar, J.M., Horstwood, M.S.A., Morris, G.A., Nasdala, L., and Norberg, N., 2008, Plešovice zircon—A new natural reference material for U–Pb and Hf isotopic microanalysis: Chemical Geology, v. 249, no. 1–2, p. 1–35, https://doi.org/10.1016/j.chemgeo.2007.11.005.

Söderlund, U., Patchett, P.J., Vervoort, J.D., and Isachsen, C.E., 2004, The $^{176}Lu$ decay constant determined by Lu–Hf and U–Pb isotope systematics of Precambrian mafic intrusions: Earth and Planetary Science Letters, v. 219, no. 3–4, p. 311–324, https://doi.org/10.1016/S0012-821X(04)00012-3.

Strickland, A., Miller, E.L., and Wooden, J.L., 2011, The timing of Tertiary metamorphism and deformation in the Albion–Raft River–Grouse Creek metamorphic core complex, Utah and Idaho: The Journal of Geology, v. 119, no. 2, p. 185–206, https://doi.org/10.1086/658294.

Taylor, J., Stevens, G., Armstrong, R., and Kisters, A.F.M., 2010, Granulite facies anatexis in the Ancient Gneiss Complex, Swaziland, at 2.73 Ga: Mid-crustal metamorphic evidence for mantle heating of the Kaapvaal Craton during Ventersdorp magmatism: Precambrian Research, v. 177, no. 1–2, p. 88–102, https://doi.org/10.1016/j.precamres.2009.11.005.

Thrane, K., 2002, Relationships between Archaean and Palaeoproterozoic crystalline basement complexes in the southern part of the East Greenland Caledonides: An

ion microprobe study: Precambrian Research, v. 113, no. 1–2, p. 19–42, https://doi.org/10.1016/S0301-9268(01)00198-X.

Vermeesch, P., 2018, IsoplotR: A free and open toolbox for geochronology: Geoscience Frontiers, v. 9, no. 5, p. 1479–1493, https://doi.org/10.1016/j.gsf.2018.04.001.

Verts, L.A., Chamberlain, K.R., and Frost, C.D., 1996, U-Pb sphene dating of metamorphism: The importance of sphene growth in the contact aureole of the Red Mountain pluton, Laramie Mountains, Wyoming: Contributions to Mineralogy and Petrology, v. 125, no. 2–3, p. 186–199, https://doi.org/10.1007/s004100050215.

Vervoort, J.D., and Blichert-Toft, J., 1999, Evolution of the depleted mantle: Hf isotope evidence from juvenile rocks through time: Geochimica et Cosmochimica Acta, v. 63, no. 3–4, p. 533–556, https://doi.org/10.1016/S0016-7037(98)00274-9.

Vervoort, J.D., and Kemp, A.I.S., 2016, Clarifying the zircon Hf isotope record of crust–mantle evolution: Chemical Geology, v. 425, p. 65–75, https://doi.org/10.1016/j.chemgeo.2016.01.023.

Vervoort, J.D., Patchett, P.J., Söderlund, U., and Baker, M., 2004, Isotopic composition of Yb and the determination of Lu concentrations and Lu/Hf ratios by isotope dilution using MC-ICPMS: Geochemistry, Geophysics, Geosystems, v. 5, no. 11, https://doi.org/10.1029/2004GC000721.

Vervoort, J.D., Lewis, R.S., Fisher, C., Gaschnig, R.M., Jansen, A.C., and Brewer, R., 2016, Neoarchean and Paleoproterozoic crystalline basement rocks of north-central Idaho: Constraints on the formation of western Laurentia: Geological Society of America Bulletin, v. 128, p. 94–109, https://doi.org/10.1130/B31150.1.

Villeneuve, M.E., Ross, G.M., Thereiault, R., Miles, W., Parrish, R.R., and Broome, J., 1993, Tectonic subdivision and U-Pb geochronology of the crystalline basement of the Alberta Basin, Western Canada: Geological Survey of Canada Bulletin, v. 447, p. 1–86, https://doi.org/10.4095/77642.

Voice, P.J., Kowalewski, M., and Eriksson, K.A., 2011, Quantifying the timing and rate of crustal evolution: Global compilation of radiometrically dated detrital zircon grains: The Journal of Geology, v. 119, no. 2, p. 109–126, https://doi.org/10.1086/658295.

Wan, Y., Liu, D., Wang, S., Yang, E., Wang, W., Dong, C., Zhou, H., Du, L., Yang, Y., and Diwu, C., 2011, ~2.7 Ga juvenile crust formation in the North China Craton (Taishan-Xintai area, western Shandong Province): Further evidence of an understated event from U–Pb dating and Hf isotopic composition of zircon: Precambrian Research, v. 186, no. 1–4, p. 169–180, https://doi.org/10.1016/j.precamres.2011.01.015.

Wang, D., Vervoort, J.D., Fisher, C.M., Lewis, R.S., and Buddington, A., 2022, The Neoarchean and Paleoproterozoic crustal evolution of the Clearwater block, northwestern Laurentia: Implications for the assembly of supercontinents: Precambrian Research, v. 379, https://doi.org/10.1016/j.precamres.2022.106780.

Whitehouse, M.J., Kamber, B.S., and Moorbath, S., 1999, Age significance of U–Th–Pb zircon data from early Archaean rocks of west Greenland—A reassessment based on combined ion-microprobe and imaging studies: Chemical Geology, v. 160, no. 3, p. 201–224, https://doi.org/10.1016/S0009-2541(99)00066-2.

Whitmeyer, S.J., and Karlstrom, K.E., 2007, Tectonic model for the Proterozoic growth of North America: Geosphere, v. 3, p. 220–259, https://doi.org/10.1130/GES00055.1.

Wiedenbeck, M., Alle, P., Corfu, F., Griffin, W.L., Meier, M., Oberli, F., Von Quadt, A., Roddick, J.C., and Spiegel, W., 1995, Three natural zircon standards for U-Th-Pb, Lu-Hf, trace element and REE analyses: Geostandards Newsletter, v. 19, no. 1, p. 1–23, https://doi.org/10.1111/j.1751-908X.1995.tb00147.x.

Wilde, S.A., Valley, J.W., Peck, W.H., and Graham, C.M., 2001, Evidence from detrital zircons for the existence of continental crust and oceans on the Earth 4.4 Gyr ago: Nature, v. 409, no. 6817, p. 175–178, https://doi.org/10.1038/35051550.

Woodhead, J.D., and Hergt, J.M., 2005, A preliminary appraisal of seven natural zircon reference materials for in situ Hf isotope determination: Geostandards and Geoanalytical Research, v. 29, no. 2, p. 183–195, https://doi.org/10.1111/j.1751-908X.2005.tb00891.x.

Worthington, L.L., Miller, K.C., Erslev, E.A., Anderson, M.L., Chamberlain, K.R., Sheehan, A.F., Yeck, W.L., Harder, S.H., and Siddoway, C.S., 2016, Crustal structure of the Bighorn Mountains region: Precambrian influence on Laramide shortening and uplift in north-central Wyoming: Tectonics, v. 35, no. 1, p. 208–236, https://doi.org/10.1002/2015TC003840.

Zartman, R.E., and Reed, J.C., Jr., 1998, Zircon geochronology of the Webb Canyon gneiss and the Mount Owen quartz monzonite, Teton Range, Wyoming: Significance to dating late Archean metamorphism in the Wyoming Craton: The Mountain Geologist, v. 35, p. 71–77.

Zhao, G., Cawood, P.A., Wilde, S.A., and Sun, M., 2002, Review of global 2.1–1.8 Ga orogens: Implications for a pre-Rodinia supercontinent: Earth-Science Reviews, v. 59, no. 1–4, p. 125–162, https://doi.org/10.1016/S0012-8252(02)00073-9.

Science Editor: Mihai Ducea
Associate Editor: Jean Bédard

Manuscript Received 31 May 2023
Revised Manuscript Received 28 August 2023
Manuscript Accepted 8 September 2023